POLITECNICO DI TORINO
Master's degree in Electronic Engineering

Thesis

IoT for 5G: candidate coding schemes

Author
Manuel Ligurgo

Supervisor
Roberto Garello
David Gómez Barquero

A.Y. 2017/2018

Abstract

The next coming 5G technology is envisioned to support multiple services and applications that will emerge in the upcoming years. These 5G applications are grouped by the International Telecommunications Union (ITU) in three broad use case families: enhanced Mobile Broadband (eMBB), massive Machine Type Communications (mMTC) and Ultra Reliable Low-Latency communications (URLLC). From the three families, mMTC, also called Internet of Things (IoT) defines the communication between objects, like smart metering, wearables, logistics and body sensors. Hence, they can be categorized as low-cost, massive in number and power-constrained. In addition, a coverage extension compared with other families is required, since they are commonly deployed in indoor environments. Any system that aims at receiving the 5G term from ITU, i.e. to be defined as IMT-2020 system, has to fulfill all the different requirements defined in its framework. In particular, the 3GPP is planning to present as their 5G candidates to ITU the New Radio (NR) Rel'15 for eMBB family, the upcoming NR Rel'16 for URLLC and the former LTE-based Rel'14 for mMTC candidate. This thesis work defines a NR-based IoT system, which could be considered for following 3GPP releases. In particular, different channel coding schemes for a potential NR-IoT solution are proposed and evaluated, i.e. *Polar code*, *Low-Density Parity Check (LDPC)*, *Turbo code* and *Tail Biting Convolutional Codes (TBCC)*. After these evaluations, a link-budget analysis has been conducted in order to estimate the Maximum Coupling Loss (MCL) that the different configurations can actually provide. The goal of evaluation was to show that the downlink channel of 5G-NR based IoT system under evaluation could support extremely deep coverage condition at 164 dB MCL with at least a data rate of 160 bps as it is specified in the ITU framework.

Resumen

La próxima tecnología venidera 5G está pensada para admitir múltiples servicios y aplicaciones que surgirán en los próximos años. Estas aplicaciones 5G están agrupadas por la Unión Internacional de Telecomunicaciones (ITU) en tres amplias familias de casos de uso: banda ancha móvil mejorada (eMBB), comunicaciones masivas tipo máquina (mMTC) y comunicaciones ultra confiables de baja latencia (URLLC). De las tres familias, mMTC, también llamado Internet of Things (IoT), define la comunicación entre los objetos, como la medición inteligente, los wearables, la logística y los sensores corporales. Por lo tanto, se pueden categorizar como de bajo costo, en cantidad masiva y con restricciones de energía. Además, se requiere una extensión de cobertura en comparación con otras familias, ya que comúnmente se implementan en entornos interiores. Cualquier sistema que aspire a recibir el término 5G de la ITU, es decir, que se defina como sistema IMT-2020, debe cumplir todos los requisitos diferentes definidos en la llamada. En particular, el 3GPP está planeando presentar como sus candidatos 5G a la ITU el sistema New Radio (NR) aprobado en la Rel'15 para la familia eMBB, la próxima Rel'16 de NR para URLLC y la anterior Rel'14 basada en LTE para mMTC. Este trabajo de tesis define un sistema de IoT basado en NR, que podría considerarse para las subsiguientes versiones de 3GPP. En particular, se proponen y evalúan diferentes esquemas de codificación de canal para una posible solución NR-IoT.

Contents

List of Figures

List of Tables

Chapter 1

Introduction

1.1 Next Generation cellular systems

After several years of research on the 5th Generation (5G) of cellular communication, it is envisioned that 5G will support diverse applications and services that recently are emerging. When 4G-LTE came out, the main use case was Mobile BroadBand (MBB) and its design focused to fulfil the high-speed Internet access for mobile users. In the meantime, technology has evolved and many other applications today are considered. These applications are characterized by different requirements with respect to the MBB and they should follow a different design. My thesis focuses the attention on the Machine Type Communication (MTC) applications, known also as Internet of Things (IoT) that are power-constrained, require only little bandwidth, extreme coverage and a network that supports a massive number of devices connected. However, they can get long data-transfer delays. Thus, the key challenges are enable a sporadic communication and long idle times as power efficient as possible. On the other hand, the vehicle-to-vehicle communication application must be very time sensible and its design goal is rather to get very low latency and high reliable communication than power consumption. Furthermore, as overall bandwidth demands and individual data rate requirements keep rising, new frequency bands need to be tapped to create an evolution path for the mobile broadband use case as well.[2]
The current LTE technology is not able to fully address non-mobile broadband scenarios, thus in the next coming generation cellular system it will expect to have a flexibility built in from the radio interface to the core network, such to achieve flexible numerology, latency-optimized frame structure, massive MIMO, interworking between high and low frequency bands and ultra-lean transmissions. This will allow to bring together people along with things, data, applications, transport systems and cities in a smart networked communications environment.

In 2012, the International Telecommunication Union occupied for Radiocommunication developing (ITU-R) started working on a programme to develop IMT-2020, setting the stage for 5G research activities that was emerging around the world. The vision of IMT-2020, released in *RECOMMENDATION ITU-R M.2083-0* [3], establishes three different families:

- Enhanced Mobile BroadBand (eMBB) addresses the human-centric uses cases for access to multi-media content,services and data
- Ultra-reliable and low latency communications (URLLC) has stringent requirements for capabilities such as throughput, latency and availability.
- Massive machine type communications (mMTC) characterized by a very large number of connected devices typically transmitting a relatively low volume of non-delay-sensitive data. Devices are required to be low cost, and have a very long battery life.

Further use cases may emerge, which are currently not foreseen. [4]

IMT for 2020 and beyond is envisioned to provide farther enhanced capabilities than those described in Recommendation ITU-R M.1645, and these enhanced capabilities could be regarded as new capabilities of future IMT. They are reported in the tab.1.1.

Key capabilities	**Description**	**IMT-2020 scenario**
Peak data rate	The maximum achievable data rate under ideal conditions per user/devices	eMBB
User experience data rate	the achievable user/device data rate across the coverage area	eMBB
Latency	The time required for a data packet to travel from the source to the destination	eMBB URLLC
Mobility	maximum mobile station speed at which a defined QoS is guaranteed	eMBB URLLC
Connection density	The total number of connected devices per area	mMTC
Energy efficiency	Capability of set of radio interface technologies to reduce the RAN energy consumption with respect to the traffic capacity provided	mMTC
Reliability	The percental of successful transmitted amount of traffic within a given time period	URLLC
Area traffic capacity	the total traffic throughput served per geographic area	eMBB

Table 1.1: Capabilities of IMT 2020

For Enhanced Mobile Broadband (eMBB) usage scenario, the 100 Mbps user experience data rate and area traffic capacity of 10 Mbps/m^2 are expected with the support of large bandwidth and 3 times spectral efficiency improvement as compared to 4G systems. These capabilities should be reached while retaining sustainable energy consumption levels. Mobility is also important and should be improved to support devices moving with speeds as high as 500 km/h. For Massive Machine Type Communications (mMTC) usage scenario, connection density is expected to reach 1,000,000 devices per km^2 due to the demand of connecting vast number of devices over the next decade. For Ultra Reliable Low Latency (URLLC) usage scenario, the 1 ms latency with very high (99.999%) reliability has been put forward as a design goal[5].

It is evident that a telecommunication system belonging to a given family is characterized by completely different features with respect to one belonging to other. Thus, a generic telecommunication 5G system does not have to respect all of key capabilities. Basically, each family is designed to support some of them, fulfilling their minimum requirements. Any system that aims at receiving the 5G term from ITU, i.e. to be defined as IMT-2020 system, has to fulfil all the different requirements defined in its framework, evidenced in the technical report [6].

1.1.1 5G use cases

The next coming generation network will address a number of very different applications, depending on which uses cases are to be addressed by individual network operators, radio network will be structured in different ways. Many uses cases have been discussed in the industry and some of them are listed here [7]:

Cloud Virtual and Augmented Reality (AR). The AR is the integration of digital information with the user's environment in real time. The bandwidth requirements needed to operate effectively are considerable and rendering can take up a huge amount of processing power in the device. Much of this rendering could be carried out in the cloud, but there is still the need to deliver high quality imaging with some applications needing in excess of 100 Mbps.

Connected Automotive. The automotive industry is moving quickly to support and test autonomous driving and in some cases autonomous cars will require ultra-low latency communications (ULLC) to support V2X (Vehicle to Everything).

Smart Manufacturing. Smart robotics and lean engineering are at the heart of Industry 4.0 and mobility is taking a foothold in the workplace in areas such as manufacturing, supply and asset management/tracking. Mobility is enabling real-time access to mission critical data and Artificial Intelligence is being used to speed up processes, improve industry performance and increase productivity.

Connected Drones. Unmanned Aerial Vehicles (UAV) are ideal products for 5G with often a need for real time video to support traffic surveillance, crime prevention or emergency support – in case of a major fire for instance. UAVs will need a 5G connection to validate parcel deliveries, potentially using facial recognition to ensure delivery to the right location and person.

Smart Cities. The idea is to give information and to incorporate communication technologies to improve the quality and performance of urban services such as parking, lighting, traffic flow, refuse collection, floods, pollution monitoring and fly tipping. This will lead to a reducing of resources, wastage and overall costs. An high resolution cameras may be at the heart of the Smart City and many may need the bandwidth of 5G to deliver high resolution imaging.

Smart Home. Every device in the house is connected to the Internet and can make decisions autonomously based on information originating from sensors, thereby contributing and improving on the personal lifestyle of end-users which makes it easier to monitor and control home appliances and systems [8].

1.2 5G New Radio

The 3GPP has specified a new fifth generation(5G) radio interface as New Radio(NR). It will describe the new 5G air interface and the required functions for interfacing the Core Network and other 3GPP air interface. To reach the 5G vision defined by ITU-R, 3GPP has further studied the deployment scenarios and the related requirements associated with the three usage scenarios. The 3GPP requirements complement the ITU requirements, defining relevant metrics to the usage scenario as it is shown on the technical report [9]. This report provides guidelines for the procedure, the methodology and the criteria to be used in evaluating the candidate IMT-2020 radio interface technologies (RITs)or set of RIT (SRITs) for a number of test environments. The evaluation procedure is designed in such a way that the overall performance of the candidate RITs/SRITs may be fairly and equally assessed on a technical basis. It ensures that the overall IMT 2020 objectives are met.

For NR, the relevant releases are Rel' 14, 15. In Rel' 14, a number of preliminary activities were done to prepare for the specification of 5G. For instance, one study was carried out to develop propagation models for spectrum above 6 GHz. Another study was done on scenarios and requirements for 5G and concluded at the end of 2016. In addition, a feasibility study was done of the NR air interface itself, generating a number of reports covering all aspects of the new air interface. Rel' 15 will contain the specifications for the first phase of 5G. The process for this specification is somewhat unusual with two «drops» to match the deployment plans of the operators. The first drop of the standard was largely completed at the end of 2017 and contains specifications of all functions necessary to enable non-standalone operation. In this drop the NR carriers are used in combination with LTE carriers in a dual connectivity manner, allowing to postpone the development of some functions and procedures and speed up the development of the standard. The functions for standalone operation will take more time to develop and the complete specification of NR is expected for the second half of 2018.

Regarding the next coming releases, it will expect that Rel' 16 will begin during the second half on this year and last until 2019 with the specification of the second phase of 5G. This release will develop the URLLC type of service as well[10]. Whereas, the Rel' 17 may be dealing with a 5G NR based IoT system.

The 3GPP is planning to present as their 5G candidates to ITU the New Radio (NR) Rel'15 for eMBB family, the upcoming NR Rel'16 for URLLC and the former LTE-based Rel'14 for mMTC candidate.

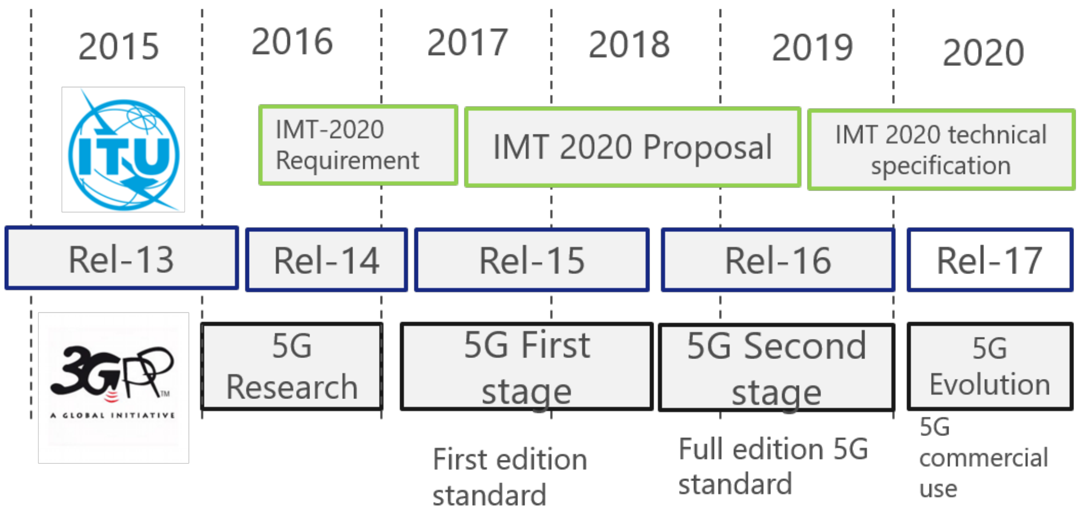

Figure 1.1: 5G NR standardization

1.3 Internet of Things and Machine Type Communication

The term Internet of Things (IoT) is coined for the first time by Kevin Ashton, a english engineer in 1999. The concept focused on guarantee that any physical object in the world is connected to a common interface with ability to communicate with each other. IoT enables the communication among machine without human intervention, known as Machine Type Communication (MTC) or Machine To Machine (M2M). Basically, each connected object contains a embedded technology that sense or interact with the internal state or external environment. According to forecasts from Ericsson [11], it is estimated that about 28 billion of smart devices will be connected across the global world by 2021, with more than 15 billion of these devices to be connected through M2M and consumer electronics devices. Research has also shown that roughly 7 billion of these devices will be connected by cellular technologies such as 2G, 3G and 4G which are currently being used for IoT but not fully optimized for IoT applications and Low-Power Wide-Area (LPWA) technology and with a revenue of about 4.3 trillion dollars [12] to be generated across the entire IoT sector globally. The current demand for Machine-Type Communications (MTC) applications such as smart community, smart building and surveillance, smart cities, smart grid, remote maintenance and monitoring systems, and smart water system etc., has brought about massive connected devices which pose a major research issue in terms of capacity for currently deployed and future communication networks.

In developing applications to implement MTC technologies, there are considerations that need to be taken into account[8]:

- According the foreseen, the number of connected smart devices will reach billions over cellular IoT technologies. Thus, it is expected that LPWA IoT connectivity solutions should be able to handle most of these connected smart devices simultaneously.

- IoT devices are *resource-constrained* and characterized by low capabilities in terms of both computation and energy capacity. So, they should include some energy save mechanism or low power operations that reduce the power consumption in order to guarantee a *long battery life*. This should be one of the most important basics of IoT enablers because, often these devices are installed to inaccessible regions and the replacing or recharging of the battery is basically not feasible. Consequently, these devices are expected to last and to be reliable for a specific number of years. To improve this autonomy, energy harvesting is taken in account as well.

- *Low device cost* and low deployment-cost are others key challenge for IoT. It is expected that the total cost of production of devices including that of ownership should be extremely very low to aid the massive deployment of IoT use cases moreover the entire network of IoT connectivity should be kept at a minimum cost, by using software upgrade on existing cellular networks to deploy LPWA IoT connectivity solution. This reduces the entire cost of new hardware and site planning.

- *Extended coverage* is the key challenge to ensure deeper coverage also for indoor employment. A promising technique for IoT connectivity link budget for coverage enhancement is being targeted to increase the existing Maximum Coupling Loss (MCL) between the device (UE) and the base station to a maximum of 164 dB.

1.3.1 Current solutions for IoT

LTE has never designed to be extremely power efficient, to handle billions of IoT devices per cell and support small packet transmission. Accordingly, 3GPP has committed over the last years to accommodate these new requirements and specify new device categories, such that each of them is addressed for a different case. E.g. Some IoT applications might want to transmit data quite frequently and at a bit-rate of a few hundred kilobits per second while a compromise can be made on power efficiency and indoor coverage in return. Other IoT devices might want to exchange only a few bytes a day but must do so from a considerable distance from a base station or may be installed in a basement where the 10 or 20 MHz channels used by LTE today simply do not reach [2]. In the following list, the categories devices are specified and briefly described:

- LTE Category 1 (Cat-1).

  This devices category has been defined by 3GPP with Rel'8 and it was the first version of the 3GPP LTE specification that offered a simpler and more power efficient communication due to complexity reducing and the employed of a single antenna. i.e. without MIMO capabilities. In addition, it offers speeds up to 10 Mbit/s.

- LTE Category 0 (Cat-0).

  Some years later, 3GPP defined this category in Rel' 12 to further stripped down by limiting the supported data-rate to 1 Mbit/s and using a half-duplex transmission. This leads to reduce cost, complexity and power consumption by replacing duplex filters with a transmit/receive switch. Thus, this device cannot send and receive at the same time. Furthermore, the Power Save Mode (PSM) was introduced to further extends the battery life of devices.

  It extends the LTE specifications with an additional radio interface state. Previously a device could either have established a radio connection to the network (RRC connected) or could be not physically connected (RRC idle) while remaining logically connected and keeping its IP address. Even if not connected a device can still receive data as the network sends a Paging message to wake it up. PSM extends this scheme by allowing the device to keep its IP address but to stop listening for incoming paging requests for very long durations.

  Unlike Cat-1 devices which will work in any LTE network today, Cat-0 devices were only specified in 3GPP Release 12. As a consequence a software update on the network side is required to support them [2].

- LTE Category M1 (Cat-M1)

3GPP delivered this category in Rel' 13 and allow to achieve a speed up to 1 Mbit/s with power efficiency enhancements. The previous LTE device categories have to be able to monitor control channels and receive data in a channel that can be up to 20 MHz wide. However, IoT applications does not required high data-rate, thereby CAT-M1 are capable to support a maximum channel bandwidth of 1.4 MHz and a maximum data-rate of 1 Mbit/s. Consequently, this requires a change on the physical layer of the LTE air interface, adding an control channels which are spread across only a 1.4 MHz bandwidth and visible just for this category devices. These changes lead many improvements concerning the cell range, in-house-coverage, signaling information and user data can be repeated through additional redundancy to further enhance the coverage. As for Cat-0 devices a software update on the network side is required.Without the upgrade, Cat-M1 devices will not detect a network as the new signaling channels are not broadcast.

- LTE Category NarrowBand (NB1 or NB-IoT).

  While the new device categories described above mainly added new functionalities to the existing LTE air interface, 3GPP decided to go a significant step further with the NB-IoT work item in 3GPP Release 13 to further reduce power consumption for the radio part of IoT devices. In addition this category provides better indoor coverage and accommodates a massive number of low-throughput devices (few hundred Kbit/s), with relaxed delay requirements.

  An NB-IoT channel is only 180 kHz wide, which is very small compared to mobile broadband LTE channel bandwidths of 20 MHz and in addition, backwards compatibility to LTE, GSM or UMTS is not supported. So an NB-IoT device only needs to support the NB-IoT part of the specification. Further informations about the specification of this category can be found in the 3GPP Technical Report TR 45.820: «Cellular system support for ultra low complexity and low throughput Internet of things»[13].

It is quite interesting to note that the last two categories are the most employed for the IoT applications and their usage depend mainly on the coverage, throughput, mobility and number of devices/cost of device. On the left side of the following figure 1.2,the applications that need of higher throughput and mobility are shown,i.e. wearable, object tracking and so on. These requirements are fully covered by the Cat-M1 devices. On the other hand, the city infrastructure, the utility metering, smart building and so on, require short messages and sporadic traffic, but larger coverage, guaranteed by the Cat-NB1 devices.

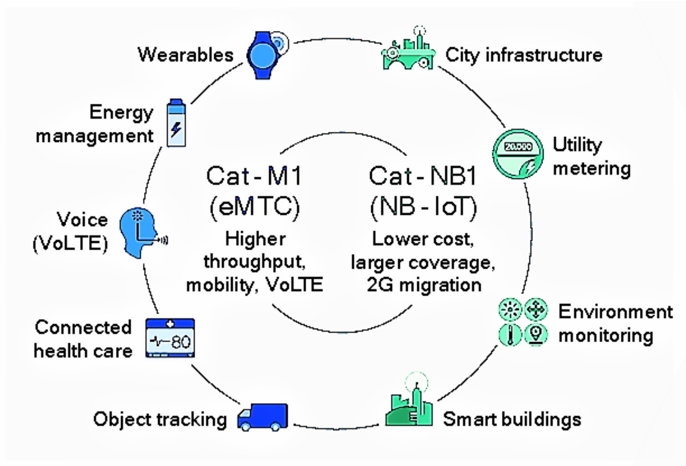

Figure 1.2: Cat-M1 and NB1 network deployment

1.4 Thesis Objective

An unprecedented variety of new applications and services are foreseen to be introduced in the next to coming 5G communication systems. This results in challenges and constraints for the envisioned usage scenarios, such as very high user data rates for eMBB services, stringent reliability and latency constraints for URLLC, or the transmission of short packet messages with sporadic traffic for mMTC. 3GPP has recently announced the 5G-NR Rel'15, which is mainly focused on enhanced Mobile Broad-Band (eMBB) family use case within IMT-2020 context, the next Rel'16 will be designed to cover the Ultra-Reliable Low Latency Communications (URLLC) family. Thus, there will be no solution of 5G NR for the massive Machine Type Communications (mMTC) before Rel'17 (2022). The 3GPP worked towards ensuring, with the Rel' 14, that further enhancements of Key Performance Indicators (KPIs) are introduced into the current LTE technologies. This is done to guarantee that the 5G mobile network is designed from scratch in order to accommodate the growing span of the IoT use cases into the market and minimizing the cost of developing new networks. Thus, this work arises to to evaluate the performance of potential 5G-NR based IoT 3GPP system. In particular, the coverage extension, one of the required gains compared with baseline 3GPP systems, has been analysed.

A special emphasis has been done on the design of Forward Error Correction (FEC) solutions in order to support efficiently the underlying constraints. In this regards, it has been taken into account the codes used in 5G-NR (Rel' 15) channels, *Low-Density Parity-Check (LDPC)* for data and *Polar code* for control, and those employed to the LTE network, *Turbo code* for data and *Tail Biting Convolutional*

Code (TBCC) for control.

The 5G-NR (Rel' 15) codes represent the state-of-the-art solutions that 3GPP identified to support the requirements of eMBB. According to the 3GPP, the LDPC represents the better choice to cope with the requirements of the different scenarios, while the Polar code has recently emerged as a strong solution for short block sizes. On the other hand, Turbo code was used in the LTE to get the target for peak data rate, but originally it has not been designed for encoding short blocks. So, the LTE FEC code does not provide capacity approaching performance for the transmission of short data packets. For this reason, it was introduced the TBCC, with tail bits for trellis terminations that tried to cope with the sporadic traffic of short messages, as typical for mMTC services.In the following chapter, the 5G-NR air interface and the candidate coding schemes will be seen more in detail. In Chapter 3, the methodology for assessing the performance of the 5G-NR based IoT air interface is described. Chapter 4 evaluates the 5G-NR based IoT air interface with the four FEC scheme previously described and with three channel models. Finally, Chapter 5 encloses the conclusion of the investigation and simulations carried out.

Chapter 2

State of the art

2.1 5G NR Radio Interface

2.1.1 Frame Structure

NR DownLink (DL) and UpLink (UL) transmissions are organized into frames. Each frame lasts 10 ms and consists on 10 subframes each of 1 ms. Since multiple OFDM numerologies are supported, each subframe can contain one or more slots. There are too 2 types of Cyclic Prefix (CP): *normal CP*, each slot conveys 14 OFDM symbols, *extended CP*, each slot conveys 12 OFDM symbols as it is shown in fig. 2.1. In addition each symbol can be assigned for DL or UL transmission, according the Slot Format Indicator (SFI), which allows flexible assignment for TDD or FDD operation modes.

In frequency domain, each OFDM symbols contains a fixed number of subcarriers. One sub-carrier allocated in one OFDM symbols is defined as one *Resource Element (RE)*. A group of 12 RE is defined as one *Resource Block (RB)*. The total number of RBs transmitted in one OFDM symbol depends on the system bandwidth and the numerology. NR supports scalable numerology for more flexible deployments covering a wide range of services and carrier frequencies. It is define a positive integer factor m that affects the sub-carrier spacing (SCS), the OFDM symbol and cyclic prefix length. NR supports the following SCSs :

$$\Delta f = 2^m \cdot 15kHz$$

where

$$m = 0{,}1{,}2{,}3{,}4$$

i.e.

$$\Delta f = 15, 30, 60, 120, 240kHz$$

A small sub-carrier spacing has the benefit of providing a relatively long cyclic prefix in absolute time at a reasonable overhead, while higher sub-carrier spacings are needed to handle, for example, the increased phase noise at higher carrier frequencies [14]. Note that the sub-carrier spacing of 15 kHz, 30 kHz and 60 kHz wide are applicable to carrier frequencies of 6 GHz or lower (sub-6), while the sub-carrier spacing of 60 kHz, 120 kHz and 240 kHz are applicable to above 6 GHz carrier frequencies[5].

Table 2.1: NR numerology (m), subcarrier spacing (SCS), useful symbol duration (Tu) and CP durations (Tcp)

m	**SCS (kHz)**	**Tu (μs)**	**Type CP**	**Tcp (μs)^2**	**Slot (μs)**	**Slots/subf**
0	15	66.66	Normal	5.2/4.7	1000	1
1	30	33.33	Normal	2.6/2.3	500	2
2	60	16.66	Normal	1.3/1.2	250	4
2	60	16.66	Extended	4.16	125	4
3	120	8.33	Normal	0.65/0.59	125	8
4	250	4.17	Normal	0.33/0.29	62.5	16

2.1.2 Downlink Physical Channels and Signals

Channels are known as flows of information transmitted between different protocol layers. Thanks to them, the different types of data are segregated and transported across different layers. In particular, physical channels carry MAC layer information, whereas physical signals are only used by the physical layer[1]. Different physical channels and signals are used in downlink and uplink transmission.

The Physical Downlink Channels and Signals are here listed and briefly described:

- *Physical Broadcast Channel (PBCH)* is used to transmit the static part of the System Information (SI), known as the Master Information Block (MIB),to all the UEs requiring to access the network and also during the beam management process.

- *Physical Downlink Control Channel (PDCCH)* is used to specify the scheduling and allocation of the data content for every UE that requests it. It also configures HARQ retransmission, link adaptation and MIMO parameters.

- *Physical Downlink Shared Channel (PBCH)*is used to transmit the data content to the UE and the System Information Blocks(SIBs)

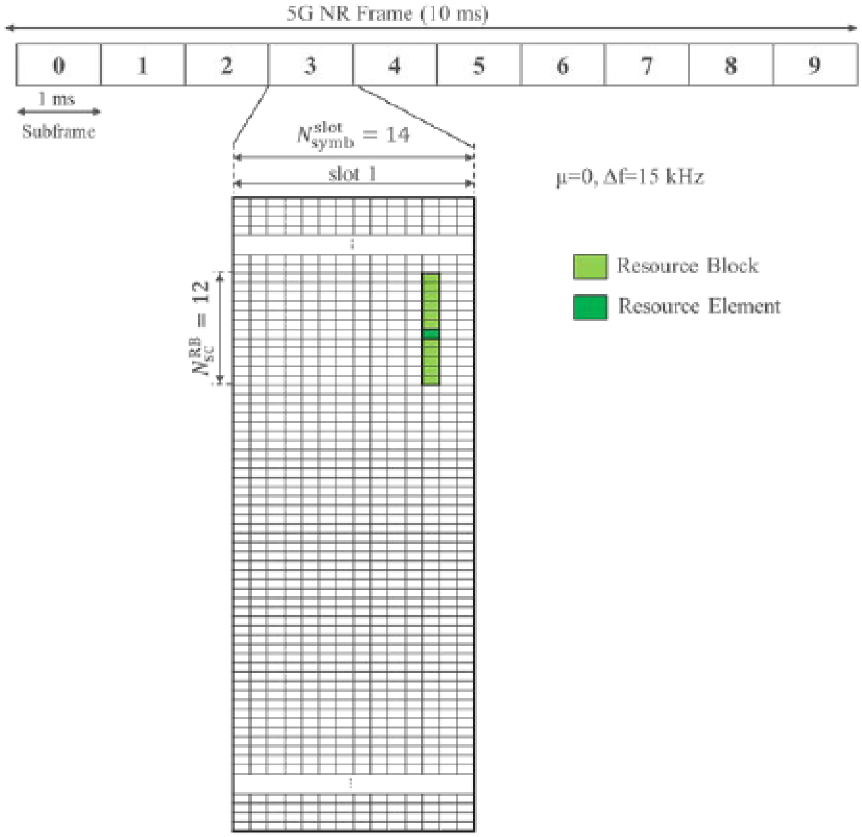

Figure 2.1: NR Framing structure for m=0

- *Primary and Secondary Synchronization Signals (PSS,SSS)* are used with PBCH to allow UE network access. They provide radio frame timing infomation and Cell ID at the initial cell search. Moreover, they are used for the beam management in IDLE state.
- *Demodulation Reference Signals (DMRS)* is used for the channel estimation and obtain the proper demodulation of PBCH,PDCCH and PDSCH.
- *Phase Tracking Reference SIgnals (PT-RS)* is used to estimate phase noise in the PDSCH in case of high frequency ranges.
- *Channel State Information Reference Signals (CSI-RS)* is used to provide channel state information (CSI), necessary for link adaptation. It is used also for beam management in CONNECTED state.

In the following figure 2.2 it is depicted how physical channel and signals are allocated in the frame structure.

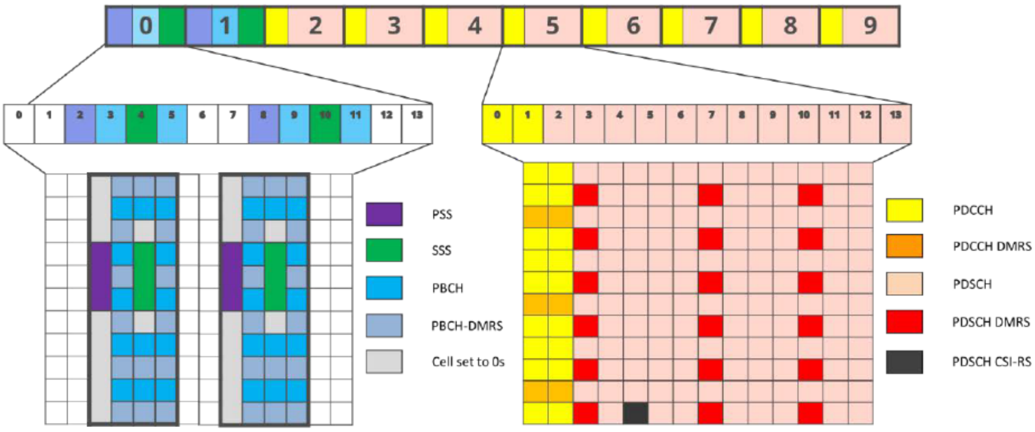

Figure 2.2: Framing structure for SFI =0

PSS, SSS, PBCH and PBCH-DMRS are grouped in SS/PBCH blocks, where each SS/PBCH block consists of 240 subcarriers and 4 OFDM symbols [15]. PSS are allocated in the first OFDM symbol while SSS are distributed across the third OFDM symbol. PBCH and PBCH-DMRS are transmitted in the second, third and fourth OFDM symbols. Cells set to 0s are used as padding to complete the block structure. There are for all the sub-carrieres with the block, m=0,1,3,4 which are selected depending on the frequency range. The allocation of SS/PBCH blocks in frequency domain depends on a high layer parameter called ssb-subcarrierOffset, while in time domain are sent in periodical burst sets andthe number of SS/PBCH blocks are sent in periodical burst depends on the numerology and the frequency band of operation.

PDCCH control information specifies the data scheduling and allocation for each UE by means of the *Downlink Control Information (DCI)*. This information is mapped within PDCCH in one or more control-channel elements (CCE). The number of CCEs allocated in the PDCCH depends on the Aggregation Level (AL), which has five possible values 1,2,4,8,16, see fig 2.3. One CCE is made up of 6 REGs, where one REG consists of one RB allocated in one OFDM symbol. REGs are mapped in control-resource sets (CORESETs) for a given numerology. The total number of REGs associated to each UE is mapped within PDCCH in CORESETs packets allocated in a specific control region. Thus, the minimum CORESET length is equal to 6 RBs x 12 REs/RB= 72 REs within a bandwidth of 1.2 MHz (i.e.m=0). While, as the fig.2.3 illustrates, taking into account AL=16, the outcome is 1152 REs. In addition, the allocation of CORESETs in frequency domain is specified by high layer parameters. Regarding the time domain allocation, CORESTEs can be transmitted at OFDM symbols 0,1 or 2 of subframes which do not contain SS/PBCH blocks.CORESET content can be distributed at most over three consecutive OFDM symblos, depending on high layer parameters. Finally, it includes DMRS signals to allow the correct demodulation of the PDCCH.

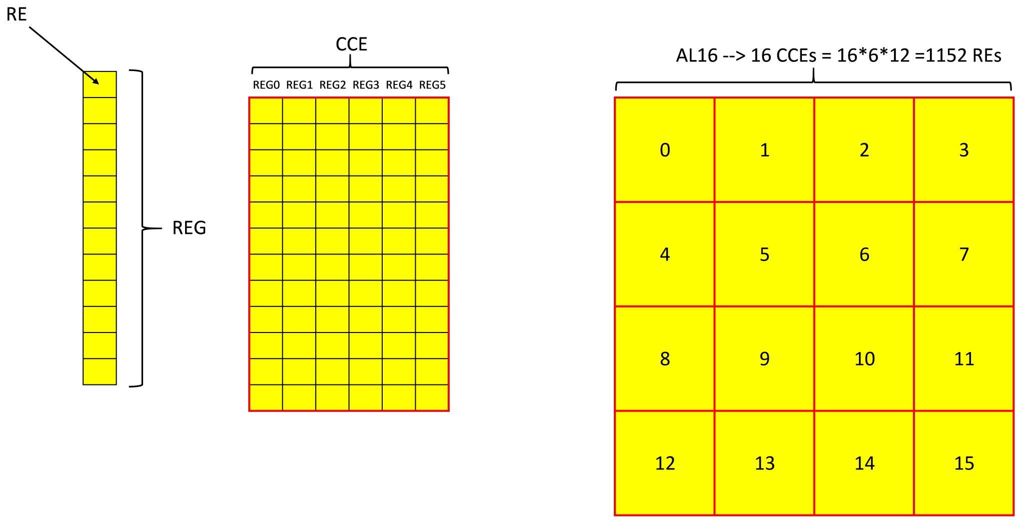

Figure 2.3: Control Channel Elements structure

PDSCH contains SIBs and data content from the higher layer DL-SCH transport channel. In particular, PDSCH is distributed in the remaining REs where the rest of channels are not allocated. The number of RBs associated to PDSCH transmissions depends on the available bandwidth and numerology. As the previous channels, it also includes DMRS in order to ease the demodulation process. DMRs allocation depends on the selected DMRs pattern. In addition, PDSCH also includes PT-RS and CSI-RS.

2.1.3 Uplink Physical Channels and Signals

The Physical Uplink Channels and Signals are here listed and briefly described:

- *Physical Random Access Channel (PRACH)*is used by the UE to request the uplink initial access and later on for beam management process.
- *Physical Uplink Control Channel (PUCCH)*carries Uplink control Information (UPI)that contains information regarding CSI,HARQ retransmission and scheduling requests.A bid difference between DCI, previously described and UCI is that the latter can be carried either by PUCCh or PUSCH depending on situation whereas DCI can be carried only by PDCCH.

- *Physical Uplink Shared Channel (PUSCH)* conveys the data content to the gNB[1].
- *Demodulation Reference Signals (DMRS)* is used for the channel estimation in order to allow the proper demodulation of PUCCH and PUSCH.
- *Phase Tracking Reference Signals (PT-RS)*is used for the same functionality than in downlink case.
- *Sounding Reference Signals (SRS)* is equivalent to CSI-RS for uplink, providing CSI to the gNB and configuring link adaptation and scheduling at the UL.

2.1.4 Acquisition Procedure

The acquisition process is a basic procedure which enables the UE connection to the network and provides basic information required to receive the data information carried in the PDSCH. The acquisition starts when UE receives the SS/PBCH block. It includes PSS and SSS, which provide frame synchronization and information of the physical cell identity. Both synchronization signals are transmitted together with PBCH. PBCH payload contains Master Information Block (MIV), which provides a minimum system information to all UEs. It also specifies the parameter configuration needed to access Remaining System Information (RMSI)CORESET, which is sent over PDCCH. RMSI CORESET carriers a special DCI which provides information about the System Information Block 1 (SIB1) scheduling. SIB1 contains information related to the availability and scheduling of other SIBs within the cell (wheter they are provided via periodic broadcast basis or only on-demand basis). SIB1 is sent over PDSCH. If the UE requests a particular SIB, PRACH uplink channel starts the initial access with Message 1 (Msg 1). Following initial access request, gNB sends random access response (Msg 2) through PDCCH and PDSCH. Then, UE requests the RRC Connection by means of Msg 3, sent via PUSCH.[16]. RRC Connection is carried through a message exchange process. Once RRC Connection has been completed, the UE acquires the Cell-Radio Network Temporary Identifier (C-RNTI), which uniquely identifies the link between the gNB and the UE. Afterwards, gNB sends in the PDCCH the DCI, which is CRC encoded and specifies where specific data is scheduled. The CRC sequence is scrambled by the C-RNTI, which disables the reception of the serving UE content for the rest of UEs. Once the DCI is decoded, the UE obtains the data allocation inside the PDSCH. Finally, the UE accedes to its corresponding

[1]gNodeB is the base station name for 5G, that replaces the eNodeB

data region, which is also scrambled with the C-RNTI. The following fig.2.4 sums up what it has been explained so far:

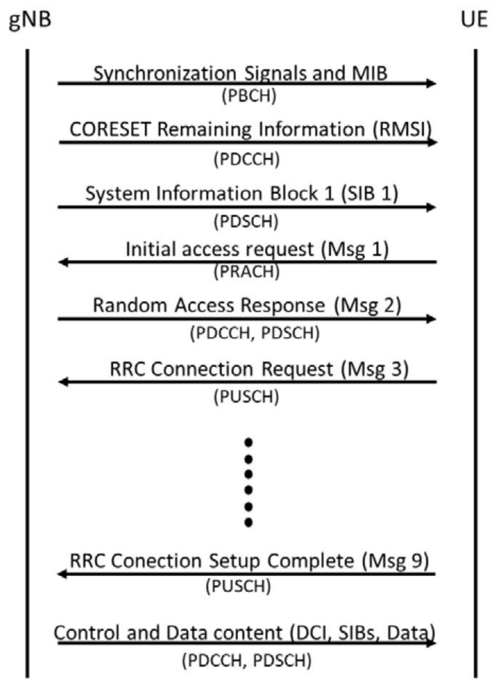

Figure 2.4: NR Rel'15 Acquisition process

Thanks to the uplink transmission, different feedback procedures can be performed, as known as Link Adaptation schemes. They are usually used: Hybrid Automatic Repeat Request (HARQ), Adaptive Modulation and Codinf (AMC) and CLose-Loop MIMO. HARQ can be used to perform physical layer retransmissions enablink transmitters to provide higher data rates for a fixed MCS selection while decreasing the number of transmitted errors. HARQ ACK are transmitted in PUCCH, while data retransmissions are sent via PDSCH.

2.2 Candidate Coding schemes

In 1948, Shannon showed that an error-free communication over a noisy channel is possible, if the information transmission rate is below or equal to a specific bound, called Channel capacity bound [17]. Since then, the efforts were focused on to find some new transmission technique with goal to approach to the channel capacity. Channel coding is one of the fundamental techniques that make it possible, by using a encoding and a decoding. The former introduces a structured redundancy at the transmitter, the latter exploit the redundancy in receiver side to detect errors and correct them.

In this section, the state of the art channel coding techniques for mMTC is reviewed. The potential requirements for this scenario are the use of lower-order modulation schemes with shorter block size information to satisfy low power requirements. The advanced channel coding schemes with robust error protection with low complexity encoding and decoding is preferred. The candidate coding scheme for the next 5G based IoT system are: *Polar code*, *Low-Density Parity Check (LDPC)*, *Turbo code* and *Tail Biting Convolutional Code (TBCC).*

2.2.1 Polar code

The *Polar code* is the state-of-art code, invented by Erdal Arikan in 2008 and used for the eMBB control channel for the 5G New Radio interface. It has attracted great interest because it can provably achieve the symmetric capacity of binary-input discrete memoryless channels under low complexity successive cancellation (SC) decoding. According his definition - The polar code can be seen as a recursive concatenation of a base short block code designed to transform the encountered transmission channel into a set of virtual channels with variable levels of reliability - [18]. The name assigned to this code derives for this feature. The channel will polarize, in the sense that some of these virtual channels will be highly reliable, and the rest will be unreliable. The idea is to put the information bits only into the reliable channels and foreknown bits into the unreliable channels. The task of polar code construction is to find this set of the most unreliable channels that are called the *Frozen Set (F)*. The encoder is basically the polarization transform, which is given by the kernel [18]:

$$T_2 = \begin{bmatrix} 1 & 0 \\ 1 & 1 \end{bmatrix}$$

The transform for a larger input length is obtained via the Kronecker product of this kernel F with itself, causing polar codes lengths that are powers of 2. For a code of N length and $n = \log_2 N$, the encoder is given by

$$G_N = T_2^{\otimes n}$$

where $T_2^{\otimes n}$ is the kronocker product of T_2 with itself n times. The following fig. 2.5 shows an example of polar encoder of length 4, according the ref.[18].

where $\vec{u} = u_1, u_2, u_3, u_4$ is the set that contain information bit and foreknown bits belonging to Frozen Set. Whereas $\vec{c} = c_1, c_2, c_3, c_4$ is given by:

$$\vec{c} = \vec{u} \times G_N$$

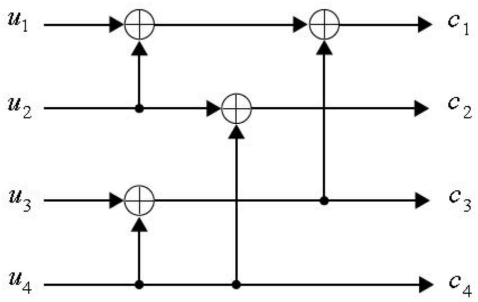

Figure 2.5: Polar encoder of length 4

Concerning the decoder side, Arikan's Successive cancellation (SC) decoder is fundamental polar decoder for achieving capacity with moderate complexity. SC decoder successively estimates the set $\hat{u}$ from receiver sequence $\vec{c}$. For each u decoder take N decisions as follows:

- if u_i is a frozen bit then decoder sets $\hat{u} = 0$;
- if u_i is information bit, calculate likelihood ratio (LLR) once estimating all previous bits.

Several modifications in the basic SC decoding algorithm have been proposed for improving finite-length performance of polar code. SC List (SCL) decoding is the most used and involves L concurrent decoding paths for significant performance improvement [19]. For each decoded bit, the two possibilities of being decoded as 1 or 0 are considered. This is achieved by splitting the current decoding path into two new paths, one for each possibility. The total number of possibilities across the decoding tree is limited by the List size. A further improvement can be achieved by performing a Cyclic Redundancy Check (CRC) on the surviving paths, and the one satisfying it, is the correct one [20].

2.2.2 LDPC

The LDPC code was first proposed by Gallager in 1960 [21] and at that time this code was considered too complex for practical implementation. In 1996, it is rediscovered and currently is used for the eMBB data channel for the 5G New Radio interface. An LDPC code is characterized by its sparse parity check matrix $H = n \times m$. Such sparsity facilitates low complexity encoding and decoding. It can be represented by a Tanner graph as it is shown in fig.2.6. Each row is represented by a check Node (CN) associated to the parity-check equation and each column is represented by a Variable Node (VN) associated to code bits. The ones in the matrix represent the connections between the CNs and VNs. In addition, the one in rows and columns should be less than n and m respectively. The encoding can be described with the following formula:

$$\vec{c} = \vec{u}\vec{G}$$

where $\vec{c}$ is the output codeword and $\vec{u}$ is the input block and $\vec{G}$ the generator matrix that is obtained from a given parity check matrix. As in the beginning it has been already said, the implementation of this code has two problems. The former is that the parity check matrix is designed for a specific input block length. This problem is solved using Quasi-Cyclick (QC) LDPC codes that support variable input size [22]. The latter lies in the transformation of H into systematic form, since it can get too complicated for long block lengths. This problem can be mitigated by utilizing a structure similar to Repeat-Accomulate (RA) codes [23].

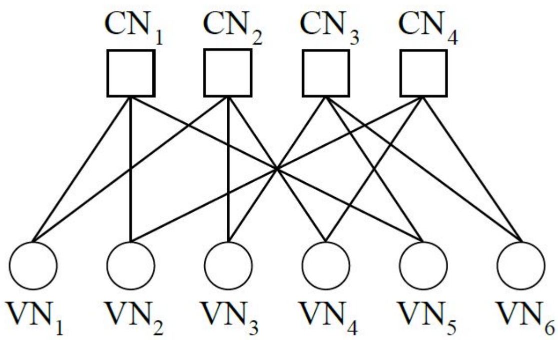

Figure 2.6: Tanner graph

LDPC codes are decoded by deploying belief propagation on a bipartite graph given by their parity check matrix. Since the Check Node operation involves multiple non-linear functions, one typically relies on sub-optimal approximations like the min-sum decoder. The scaled-min-sum decoder can reduce the approximation error due to min-sum decoding by scaling the outgoing CN messages by a constant factor.

2.2.3 Turbo code

Turbo code has been developed around 1990, but fist published in 1993 and is used in data channel in LTE mobile communications. Turbo codes are usually constructed by a parallel concatenation of two recursive convolutional encoders separated by an Interleaver. The task is then to design the code polynomials for the individual encoders, and to use an appropriate interleaver called Quadratic Permutation Polynomials (QPP) interleaver. The encoding is carried out according the fig.2.7. The outputs of the fist encoder are a systematic stream u_l, and a parity stream $p_l^{(1)}$, while the second encoder generates a parity stream $p_l^{(2)}$ only, achieving a code rate of 1/3.

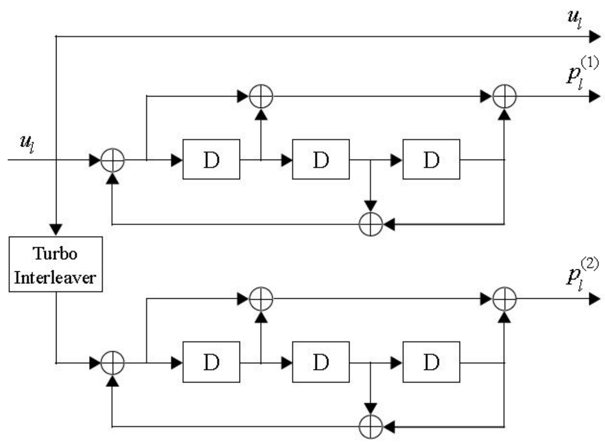

Figure 2.7: Turbo code encoder

The iterative decoders of Turbo codes rely on exchanging extrinsic information between two constituent decoders that work well with long messages. These deciders are called Soft-Input Soft-Output (SISO) decoders. The systematic stream and the fist parity stream are fed to the fist decoder, while an interleaved version of the systematic stream and the second parity stream are fed to the second one. The first decoder generate a cleared up version called extrinsic information that is interleaved and sent to the second decoder. It performs decoding with higher reliability compared to the case where it does not have the additional information from the first decoder. Therefore, it performs deinterleaving and generates a extrinsic information for the first decoder. This operation, named iteration, is performed more time, usually 8 times, in order to achieve a more reliable output.

2.2.4 TBCC

TBCC have been employed in the LTE control channels and LTE-IoT data channels, due to its low complexity encoding/decoding and outstanding performance with very short length. Firstly, the convolutional code (CC) is generated by a shift register with L=6 cells, then its trellis has 64 states. See fig. Usually, the CCs use termination, a technique which prevents the reduction of the minimum distance in the last section of the trellis. With termination L extra bits equal to 0 are transmitted to force the encoder to return to the zero state.However, these extra bits are a waste because they do not really carry data. Moreover, the true code-rate becomes different from the original 1/3. While, TBCC with respect to the convolutional codes does not require a termination which may cause a significant rate loss for short lengths and tail biting is applied. The idea is that the starting state and the final state must be the same. Since the state is determined by the last 6 bits, to do this the final 6 bits of the information message are copied inside the shift register cells before stating encoding. In the following scheme, fig.2.8 is depicted the encoder.

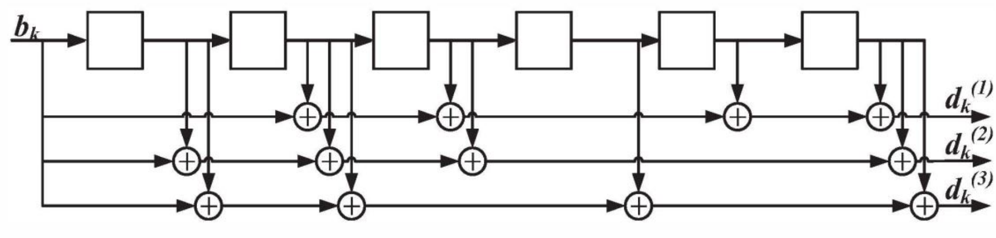

Figure 2.8: TBCC encoder

In receiver side a simple 64 state Viterbi Decoder is applied, that estimates the maximum likelihood sequence using the states of trellis representation of the code [24].

Chapter 3

Methodology

The methodology for assessing the performance of a wireless communication system is divided into two steps:

1. the assessment of the CNR threshold, conducted via *link-level simulation.* This is generally used to simulate the point-to-point physical layer technologies with propagation model taken into account. However, link-level simulation involves a single-cell and does not consider the impact of interference by near cells.

2. the estimation of the coverage area over synthetic and realistic scenarios conducted via *system level simulation.* It is an indispensable means of wireless network performance evaluation, in standardization and planning.

In this thesis, the evaluation of performance will be carried out using the link-level simulation by using a simulator designed by Universidad Politecnica de Valencia (UPV), implemented in Matlab.

3.1 Link-level simulation

A generic link level simulations can be structured in main four components: transmitter configuration, channel filtering, receiver configuration and error measurement as shown in the fig.3.1

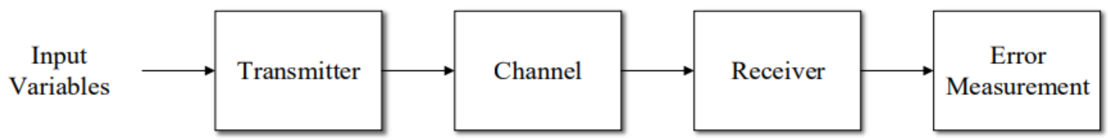

Figure 3.1: Generic link-level simulator block diagram

The 5G-NR Physical Layer simulator designed by UPV, follows basically this structure that allows maintaining high flexibility of simulation scenarios and parameter settings. In the following subsections, it will be depicted and explained each 5G-NR Link-level block.

3.1.1 Transmitter

In the transmitter block, the information bit, coming from the upper layer are channel encoded, mapped, interleaved and OFDM modulated, according to the configuration under evaluation. Fig.3.2 illustrates 5G-NR link-level transmitter block diagram.

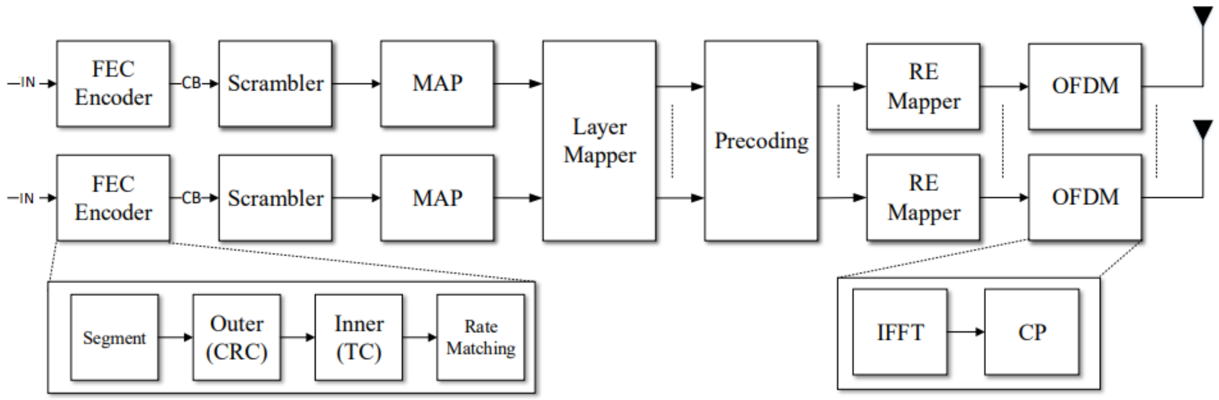

Figure 3.2: 5G NR Link-level transmitter block diagram

First of all, the FEC scheme includes more processes: the *segmentation*, *outer coding*, *inner coding* and *rate matching*. At the data information *IN* called also *Transport Block (TB)*, is attached a first *Cyclic Redundancy Check (CRC)* bit sequence. The outer coding CRC is a error detecting code that determines in receiver side if the TB was correctly transmitted. If the length of data information is longer that the system support, it is needed the segmentation. This operation consists of splitting the data information in Coded Block (CB) and attaching an additional CRC bit sequence to each of them, as the fig 3.3 shows.

The bit sequence of each CB is coded according the inner code scheme, described in the previous chapter. This operation enables reliable delivery of digital data over unreliable communication channels, adding redundancy to allow an error correction detected previously by the outer coding.

The basic function of rate matching module is to match the number of bits in transport block (TB) to the number of bits that can be transmitted in the given allocation. Basically, the bits of each TB are interleaved, circular buffered and punctured.

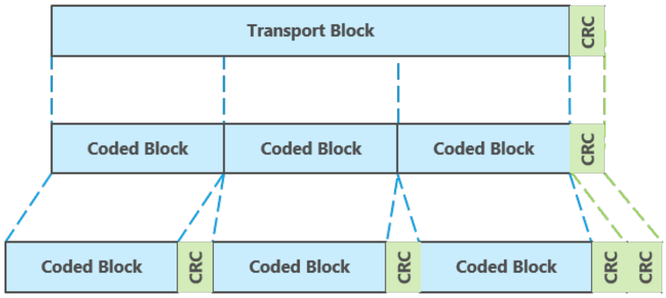

Figure 3.3: Segmentation and Outer coding (CRC)[1]

The next blocks are Scrambler and Mapper. The information coded now is scrambled for protection against burst errors and transformed (mapped) to complex symbols. The complex-valued modulation symbols are next mapped onto one or several transmission layers,i.e.*Single Input Single Output (SISO)* or *Multi Input Multi Output (MIMO)*.A MIMO precoding is applied to the mapped FEC blocks if it is desired. Finally, OFDM modulator includes the *Inverse Fast Fourier Transform (IFFT)* and *Cyclic Prefix (CP)* blocks. The former block converts the QPSK symbols from frequency domain to time domain, and the latter is used for combating InterSymbolic Interference (ISI) and InterCarrier Interference (ICI).

3.1.2 Channel

The transmitted signal is then passed through a channel that models the time and frequency variations that the transmitted signal experiences through the channel. Furthermore, in this channel there is multipath propagation that leads in receiver side to have a distorted signal. In addition, it is added noise according to the CNR under study.

Initially, the link-level evaluations are performed using the Additional White Gaussian Noise (AWGN) model, that represents a simply and useful instrument for gaining insight into the underlying behaviour of a system. In fact, the AWGN channel adds circularly symmetric complex gaussian noise with variance δ^2 to the transmitted signal. However, this channel model does not consider phenomena that occur in real scenario: fading, frequency and time selectivity and it is necessary to take into account a «real» channel model. New accurate radio propagation models are needed for the new 5G systems operating in bands up to 100 GHz. In particular, it is really important developing a channel model for these bands which are not addressed by existing channel models. In the technical report [25], study in channel model for frequencies from 0.5 to 100 GHz are reported as well as the channel models for link-level evaluations. The Tapped Delay Line (TDL) models are reported for link-level evaluations and they are classified as follows:

- TDL-A, TDL-B and TDL-C are constructed to represent channel profiles for NLOS, usually used for indoor scenario.
- TDL-D and TDL-E are constructed to represent channel profiles for LOS, usually used for outdoor.

These channel models, according the ITU [9] are also called respectively TDL-i,TDL-ii,TDL-iii, TDL-iv and TDL-v. In additional, this technical specified the TDL-iii and TDL-v as the NLOS and LOS link-level channel model for mMTC scenario, that is characterized by high density connections.

Regarding the TDL model, the doppler spectrum for each tap is characterized by a classical (Jakes) spectrum shape and a maximum Doppler shift $f_D = \vec{v}/\lambda_0$. Due to the presence of a LOS path, the first tap in the LOS model, follows a Ricean fading distribution. For those taps the Doppler spectrum additionally contains a peak at the Doppler shift $f_S = 0.7 f_D$ with an amplitude such that the resulting fading distribution has the specified K-factor. Further information about K are reported in [9]. Each TDL model can be scaled in delay so that the model achieves a desired RMS delay spread. All the detail about NLOS and LOS models are reported in the following tables 3.1 and 3.2.

Tap #	Fading distribution	TDL-i Normalized delays	Power in [dB]	TDL-ii Normalized delays	Power in [dB]	TDL-iii Normalized delays	Power in [dB]
1	Rayleigh	0.0000	-13.4	0.0000	0	0.0000	-4.4
2	Rayleigh	0.3819	0	0.1072	-2.2	0.2099	-1.2
3	Rayleigh	0.4025	-2.2	0.2155	-4	0.2219	-3.5
4	Rayleigh	0.5868	-4	0.2095	-3.2	0.2329	-5.2
5	Rayleigh	0.4610	-6	0.2870	-9.8	0.2176	-2.5
6	Rayleigh	0.5375	-8.2	0.2986	-1.2	0.6366	0
7	Rayleigh	0.6708	-9.9	0.3752	-3.4	0.6448	-2.2
8	Rayleigh	0.5750	-10.5	0.5055	-5.2	0.6560	-3.9
9	Rayleigh	0.7618	-7.5	0.3681	-7.6	0.6584	-7.4
10	Rayleigh	15.375	-15.9	0.3697	-3	0.7935	-7.1
11	Rayleigh	18.978	-6.6	0.5700	-8.9	0.8213	-10.7
12	Rayleigh	22.242	-16.7	0.5283	-9	0.9336	-11.1
13	Rayleigh	21.718	-12.4	11.021	-4.8	12.285	-5.1
14	Rayleigh	24.942	-15.2	12.756	-5.7	13.083	-6.8
15	Rayleigh	25.119	-10.8	15.474	-7.5	21.704	-8.7
16	Rayleigh	30.582	-11.3	17.842	-1.9	27.105	-13.2
17	Rayleigh	40.810	-12.7	20.169	-7.6	42.589	-13.9
18	Rayleigh	44.579	-16.2	28.294	-12.2	46.003	-13.9
19	Rayleigh	45.695	-18.3	30.219	-9.8	54.902	-15.8
20	Rayleigh	47.966	-18.9	36.187	-11.4	56.077	-17.1
21	Rayleigh	50.066	-16.6	41.067	-14.9	63.065	-16
22	Rayleigh	53.043	-19.9	42.790	-9.2	66.374	-15.7
23	Rayleigh	96.586	-29.7	47.834	-11.3	70.427	-21.6
24	Rayleigh	N/A	N/A	N/A	N/A	86.523	-22.8

Table 3.1: NLOS models TDL-i, TDL-ii, and TDL-iii

Tap #	Fading distribution	TDL-iv Normalized delay	Power in [dB]	TDL-v Normalized delay	Power in [dB]
1	LOS path	0	-0.2	0	-0.03
	Rayleigh	0	-13.5	0	-22.03
2	Rayleigh	0.035	-18.8	0.5133	-15.8
3	Rayleigh	0.612	-21	0.5440	-18.1
4	Rayleigh	1.363	-22.8	0.5630	-19.8
5	Rayleigh	1.405	-17.9	0.5440	-22.9
6	Rayleigh	1.804	-20.1	0.7112	-22.4
7	Rayleigh	2.596	-21.9	1.9092	-18.6
8	Rayleigh	1.775	-22.9	1.9293	-20.8
9	Rayleigh	4.042	-27.8	1.9589	-22.6
10	Rayleigh	7.937	-23.6	2.6426	-22.3
11	Rayleigh	9.424	-24.8	3.7136	-25.6
12	Rayleigh	9.708	-30.0	5.4524	-20.2
13	Rayleigh	12.525	-27.7	12.0034	-29.8
14	Rayleigh			20.6519	-29.2
The first tap follows a Ricean distribution with a K-factor of K1 and a mean power of 0 dB		K1 = 13.3 dB		K1 = 22 dB	

Table 3.2: LOS models TDL-iv, TDL-v

3.1.3 Receiver

In the following fig.3.4, it is depicted the block scheme of the 5G-NR receiver.

First of all, in demodulation stage, it is extracted the CP and then computed the FFT, transforming the signal in time domain to frequency domain. Then, references signals (a.k.a *pilots*) are used to estimate the noise power and the Channel Frequency Response (CFR)for each receiver antenna, in case of MIMO. The CFR values are needed for *equalization* to obtain the transmitted complex-valued symbols.

Now, this information is de-scrambled and passes through the FEC decoder part which includes: rate recover, decoder, Code Block De-segmentation and CRC decoder. Here the transmitted bits are estimated.

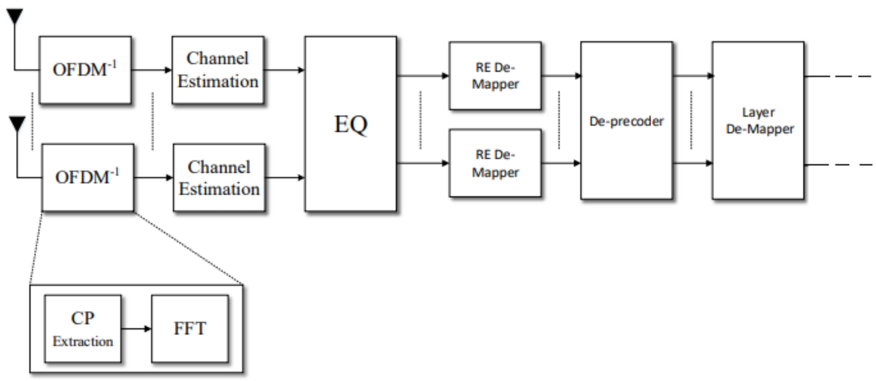

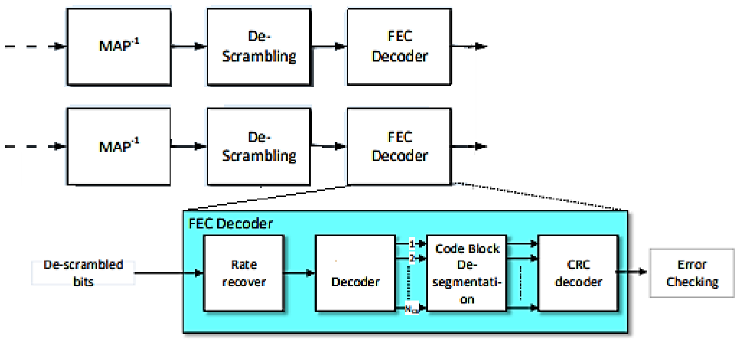

Figure 3.4: Link-level receiver block diagram

3.1.4 Error measurement

The error measurement is performed by comparing the decoded bits with transmitted bits in order to obtain Bit Error Rate (BER) and Block Error Rate (BLER) for a specific CNR.

3.2 Changes on the 5G-NR Physical Layer simulator

The 5G-NR Physical Layer simulator designed by Universidad Politecnica de Valencia (UPV) has the goal to enable performance evaluation of 5G-NR PDSCH. In fact, it includes the implementation of LDPC as FEC scheme. However, in this investigation, some modifications are done to this simulator with the aim of enabling performance evaluation of PDSCH of a future 5G-NR based IoT system. In particular, these changes involve the FEC scheme, that is the block that mainly affects the performance of the telecommunication system. In order to simplify the explanation, the following fig. 3.5 sums up the structure of the 5G-NR Physical Layer simulator and highlights the script edited.

The encoding/recovery of data is provided by the *LTE system Toolbox*, *5G Library for LTE system Toolbox* with the Matlab version R2018a, *5G Toolbox* with the last Matlab version R2018b. These toolboxes provide standard-compliant functions for the design, simulation and verification of the LTE, LTE-A and 5G as defined in the corresponding technical reports released by 3GPP. Moreover, the system toolbox accelerates the algorithms and physical layer development,

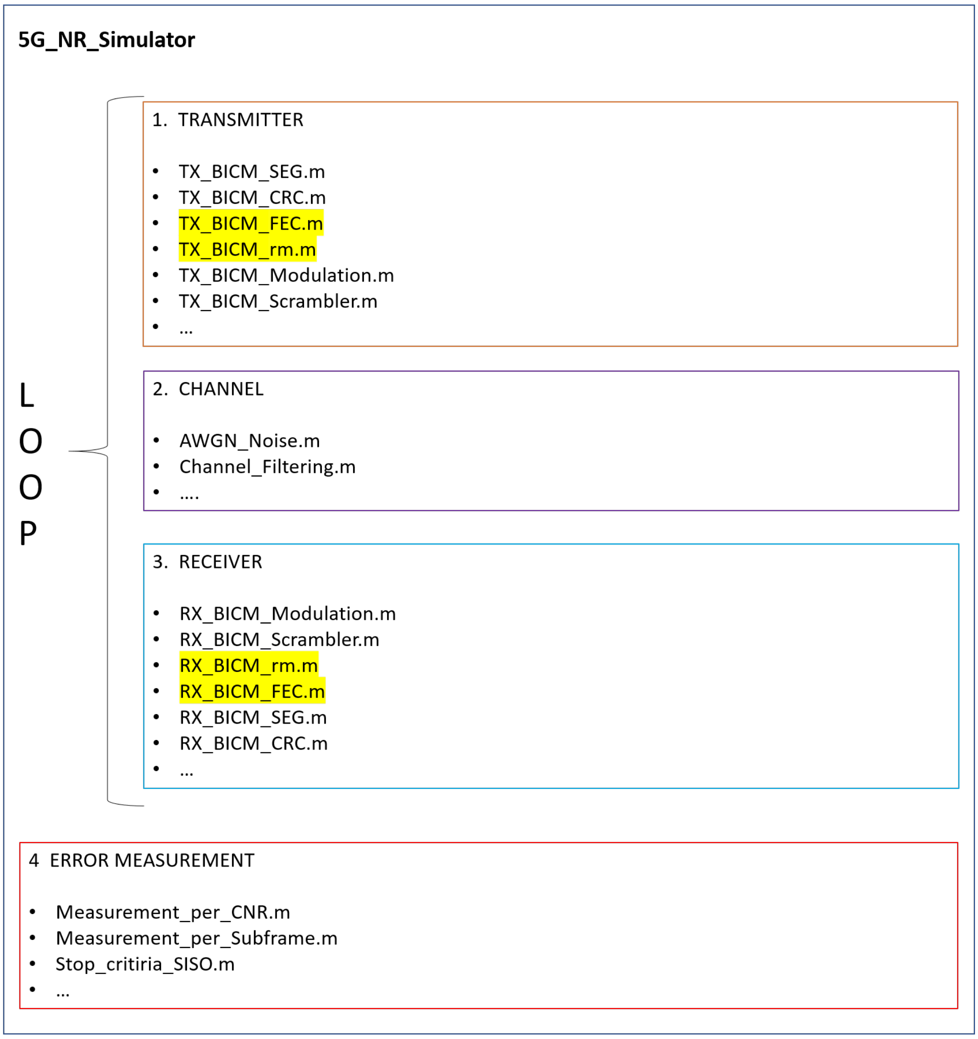

Figure 3.5: 5G-NR UPV Simulator Structure

supports golden reference verification and conformance testing, and enables test waveform generation.

In the tab. 3.2 are shown the names of the functions used in encoding and decoding phase. Instead, the tab. 3.2 refers to the rate matching and rate recover functions involved. Each of them may be looked for in Matlab to understand how actually work.

Here, an script that reports the simulation of a frame, using Polar Code as FEC scheme with the aid of 5G Toolbox of Matlab R2018b. Every function used in this script has been placed in the corresponding section of 5G-NR UPV Simulator structure above.

Inner coding	**Encoding function**	**Decoding function**
Polar	nrPolarEncode	nrPolarDecode
Turbo	lteCodeBlockSegment	lteTurboDecode
TBCC	lteConvolutionalEncode	lteConvolutionalEncode

Table 3.3: Encoder and decoder functions from Toolbox

Inner coding	**Rate Matching function**	**Rate recovery function**
Polar	nrRateMatchPolar	nrRateRecoverPolar
Turbo	lteRateMatchTurbo	lteRateRecoverTurbo
TBCC	lteRateMatchConvolutional	lteRateRecoverConvolutional

Table 3.4: Rate matching and rate recovery functions from Toolbox

```
% ------------------- Code parameters---------------------------------%
K = 36;                % Message length in bits, including CRC, K > 30
E = 312;               % Rate matched output length, E <= 8192

EbNo = 0.8;            % EbNo in dB
L = 8;                 % List length, a power of two, [1 2 4 8]
numFrames = 10;        % Number of frames to simulate
linkDir = 'DL';        % Link direction: downlink ('DL') OR uplink ('UL')

%--------------------- Polar encoding -------------------------------%

if strcmp(linkDir,'DL')
    % Downlink scenario (K >= 36, including CRC bits)
    crcLen = 24;       % Number of CRC bits for DL, Section 5.1, [6]
    poly = '24C';      % CRC polynomial
    nPC = 0;           % Number of parity check bits, Section 5.3.1.2, [6]
    nMax = 9;          % Maximum value of n, for 2^n, Section 7.3.3, [6]
    iIL = true;        % Interleave input, Section 5.3.1.1, [6]
    iBIL = false;      % Interleave coded bits, Section 5.4.1.3, [6]
else
    % Uplink scenario (K > 30, including CRC bits)
    crcLen = 11;
    poly = '11';
    nPC = 0;
    nMax = 10;
    iIL = false;
    iBIL = true;
end

```

```
%--------------------Simulate a frame--------------------------------%

 % Generate a random message
    msg = randi([0 1],K-crcLen,1);

    % Attach CRC
    msgcrc = nrCRCEncode(msg,poly);

    % Polar encode
    encOut = nrPolarEncode(msgcrc,E,nMax,iIL);
    N = length(encOut);

    % Rate match
    modIn = nrRateMatchPolar(encOut,K,E,iBIL);


    % Object constructions

    qpskMod    = comm.QPSKModulator;
    nVar = 0.3;
    chan       = comm.AWGNChannel('NoiseMethod','Variance','Variance',nVar);
    qpskDemod = comm.QPSKDemodulator('DecisionMethod', ...
        'Approximate log-likelihood ratio', 'Variance',nVar);

    % Modulate
    modOut = qpskMod(modIn);

    % Add White Gaussian noise
    rSig = chan(modOut);

    % Soft demodulate
    rxLLR = qpskDemod(rSig);

    % Rate recover
    decIn = nrRateRecoverPolar(rxLLR,K,N,iBIL);

    % Polar decode
    decBits = nrPolarDecode(decIn,K,E,L,nMax,iIL,crcLen);

    % Compare msg and decoded bits
    errStats = ber(double(decBits(1:K-crcLen)), msg);
    numferr = numferr + any(decBits(1:K-crcLen)~=msg);
```

```
disp(['Block Error Rate: ' num2str(numferr/numFrames) ...
      ', Bit Error Rate: ' num2str(errStats(1)) ...
      ', at SNR = ' num2str(snrdB) ' dB'])
```

Chapter 4

Performance evaluation

This section evaluates the 5G-NR based IoT air interface with the four FEC scheme previously described and with three channel models. The evaluations are performed in terms of the Block Error Rate (BLER) for different information block lengths (IN) and number of repetitions (AL).

Section 4.1 briefly describes the general simulation setup considered during the performance evaluation. Next, Section 4.2 evaluates the performance of the four FEC schemes in the absence of a particular fading channel, i.e. an AWGN channel. Section 4.3 and 4.4 evaluate the performance considering the recommended IMT-2020 LoS and NLoS mMTC channel models, i.e TDL-v and TDL-iii, respectively. Finally, Section 4.5 will be dedicated to understand how much coverage this telecommunication system can actually provide, using Link budget.

4.1 Simulation Setup

All simulations have assumed the following fixed configuration:

- the numerology 0, i.e. carrier spacing of 15 kHz
- bandwidth of 180 kHz (like NB-IoT)
- the Quadrature Phase Shift Modulation (QPSK)
- SISO system model

The different performance evaluations follow the description below:

- **Channel model**. Initially, the AWGN is considered, then the performance of 5G-NR based IoT is also evaluated for mMTC scenario according to the

IMT-2020 evaluation guidelines. In particular, the TDL-iii and TDL-v models are taken into account as channel models for testing a urban macro environment (UMa). They target continuous coverage focusing on a high number of connected machine type devices. For further information about TDL-iii and TDL-v, see pag.32 of [9].

- **Input size**. Since the data traffic generated by IoT applications requires small volume, it has been considered a data bit range from 12 up to 132 with a step of 12. The segmentation (and de-segmentation) block has not been considered due to small data packet to transmit. Furthermore, the information bit IN from upper layers is randomly generated and does not refer to a specific channel.

- **FEC scheme**: According the inner coding used, the information is transmitted to the next block through N bit. LDPC, Polar, Turbo-code and TBCC are assumed.

- **Aggregation Level (AL)**: The number of bits that are finally transmitted E is strictly related to the aggregation level according the following formula:

$$E = N_{ava} \cdot AL$$

where N_{ava} indicates the number of bits available to use for transmitting information in one subframe. For m = 0, the number of available resource elements in a subframe is $12 \times 14 = 168$ REs. Assuming that 12 REs are used for DMRS, the $N_{ava} = 168 - 12 = 156$. Hence, taking into account that each RE consists of 2 bits because of using a QPSK modulation, the total number of bits in one subframe is 312 bits. AL = 1, 2, 4, 8, 16 are considered. The next tab.4.1 presents the E values associated with the different AL:

AL	1	2	4	8	16
E	312	624	1248	2496	4992

Table 4.1: The E bits values related to AL

4.2 5G-NR based IoT Performance over AWGN

4.2.1 CNR vs BLER

The fig. 4.1 shows the CNR values required for each inner coding to achieve 1% BLER (equal to 10^{-2}) for IN = 12 and AL=1. It is clear that Polar code achieves a lower CNR for the fixed BLER target. LDPC and TBCC behave similarly, whereas

Turbo performs significantly worst. In particular, Polar code achieves -5,49 dB, LDPC and TBCC lose respectively only 0.8 dB and 1 dB with respect to Polar code performance. Whereas Turbo code operates worse with small data traffic, achieving -3.11 dB.

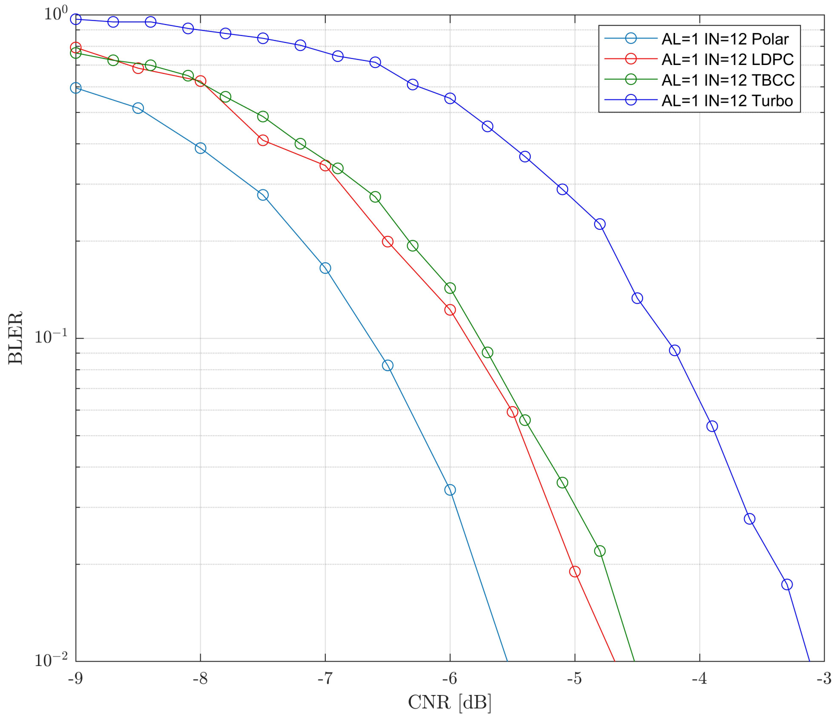

Figure 4.1: AWGN model: CNR vs BLER for IN=12 and AL=1

4.2.2 IN vs CNR

The figures 4.2 provides information on the behaviour of the four inner coding with respect to the data information length IN, considered and AL=1.

All the curves rise with the growing of associated input IN, demonstrating than they perform worse with higher data traffic. However, there are two reversals of code performance, highlighted by two crosses. The comparison of 5G NR codes showed that for short information block length, up to 96 bits, the required Carrier-to-Noise Ratio (CNR) to achieve a Block Error Rate BLER $= 10^{-2}$ is lower with Polar code, but beyond LDPC outperforms Polar. On the other hand, Turbo has a slightly growth of performance with respect to TBCC, when IN is higher than 48 bit.

However, these values strictly depend on the aggregation level considered as it will be shown on the next figures.

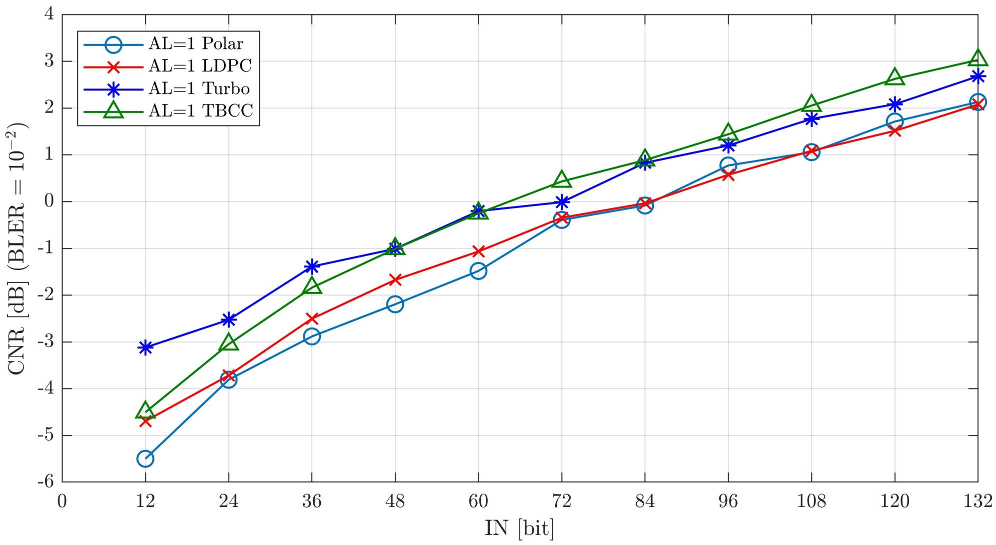

Figure 4.2: AWGN model: IN vs CNR AL=1

4.2.3 AL vs CNR

As it can be firstly observed from fig.4.3, the higher the AL, i.e. the higher the number of repetitions, the better the performance of the system. In particular, every repetition increment of power 2 allows a 3 dB performance gain. This can be proved more in detail on the tables available in the AppendixA that report the CNR values for 1% BLER for every inner codes. However, the double the AL, the half the corresponding data rate.

Moreover, in fig (a) and (d) illustrates that initially the Polar code, with IN = 12 outperforms LDPC, then when IN= 132, LDPC achieves a lower CNR. In fig (c) NR codes are overlapped when IN=96 bit, achieving the same performance. Same conclusion have been extracted between the LTE codes in fig (b), but the exchange is observed at a shorter information length. TBCC outperforms Turbo code, but the latter surpasses the former from 48 bits.

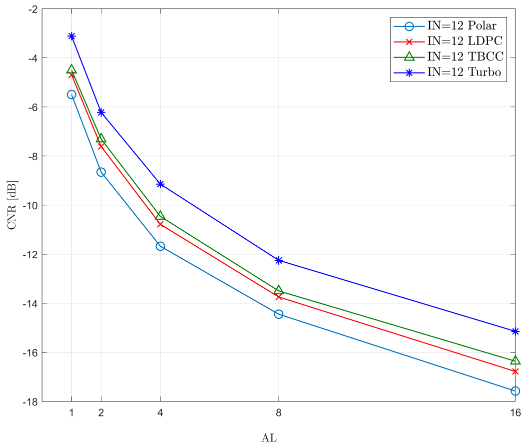

(a) IN=12 bit

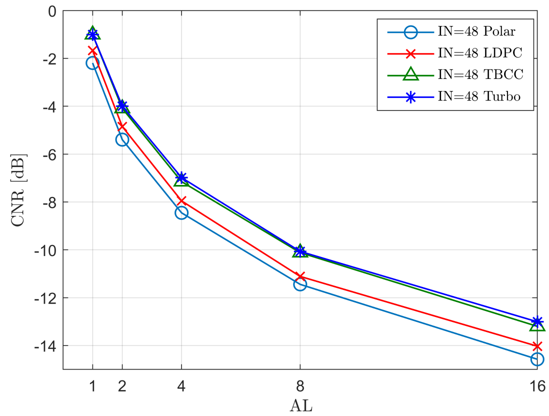

(b) IN=48 bit

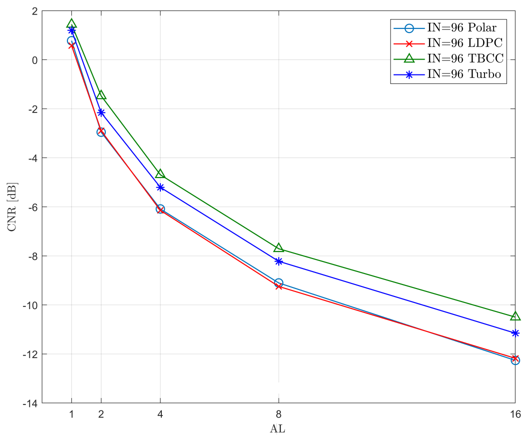

(c) IN=96 bit

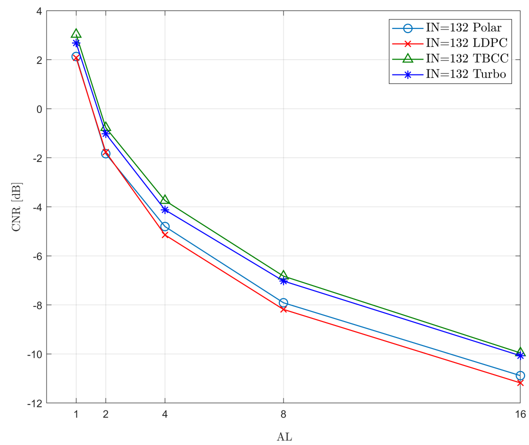

(d) IN=132 bit

Figure 4.3: AWGN model: AL vs CNR for IN=12,48,96,132

4.3 5G-NR based IoT Performance over TDL-v

4.3.1 CNR vs BLER

This section evaluates the CNR values obtained by the candidate schemes, required to achieve 1% BLER in a realistic scenario, in particular, outdoor scenario. In fig. 4.4the FEC schemes with IN=12 and AL=1 are analysed. The CNR comparison between the AWGN model and TDL-v shows how buildings in this latter model, slightly reduces the CNR performance. In fact, the tables reported in Appendix A demonstrate that the FEC schemes in outdoor scenario behave similarly to ideal scenario. The CNR value of TDL-v differ of few decimal of dB (0.1 up to 0.3 dB) with respect to AWGN model.

The Polar code keeps performing better than other codes, achieving -5.2 dB, differing only 0.3 dB with respect to the ideal scenario. It follows the LDPC, TBCC and Turbo code, with respectively -4.7 dB, -4.3 dB and -3.1 dB.

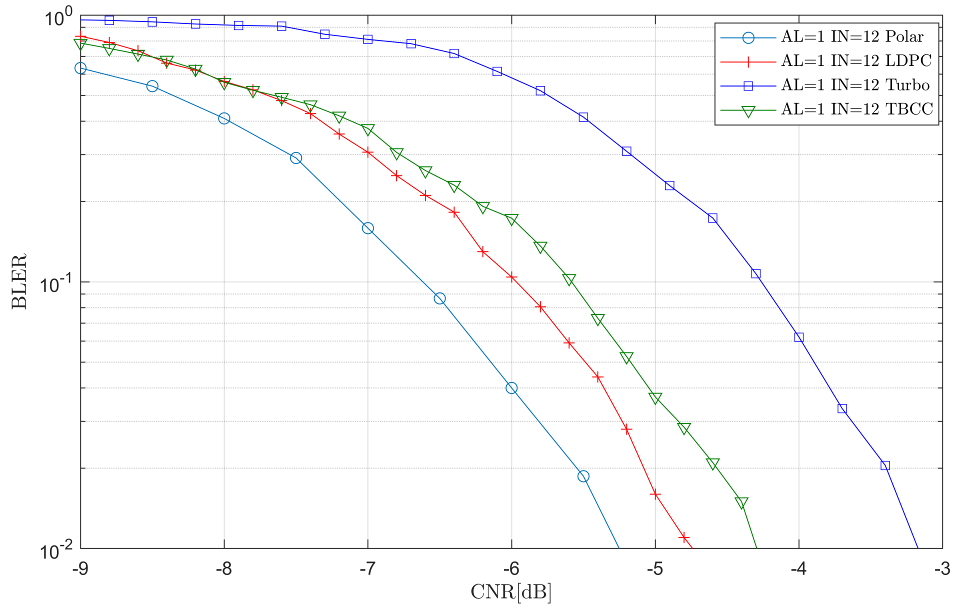

Figure 4.4: TDL-v model: CNR vs BLER for IN=12 and AL=1

4.3.2 IN vs CNR

The IN vs CNR plot is omitted, due to the imperceptible differences with respect to AWGN channel model.

4.3.3 AL vs CNR

As the AWGN case, the performance of inner coding change with respect to the input length IN, fig.4.5. In fact, these figures further demonstrate that the polar code outperforms other codes incase of small data traffic, conversely LDPC is more suitable for bigger data traffic.

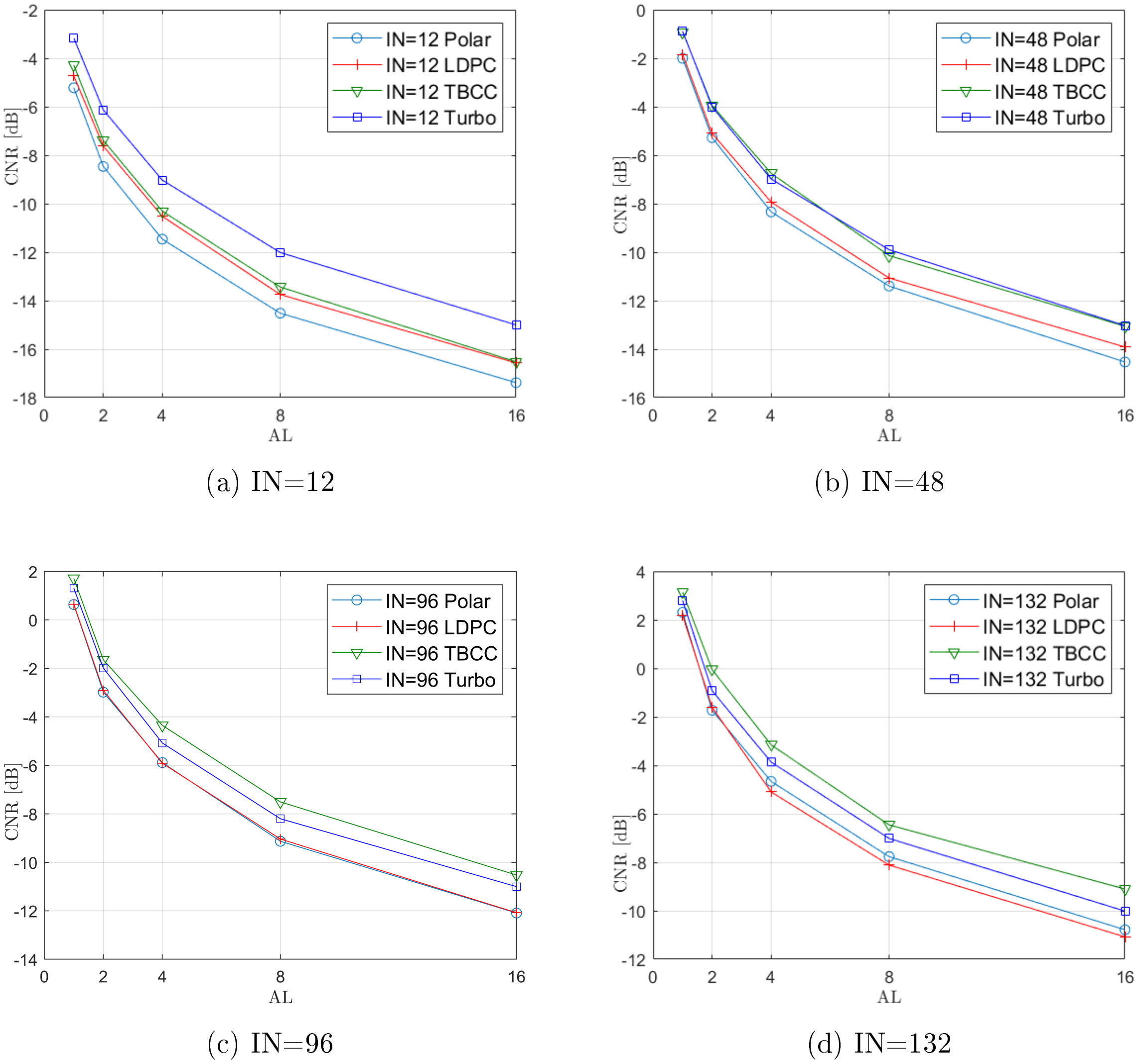

(a) IN=12

(b) IN=48

(c) IN=96

(d) IN=132

Figure 4.5: TDL-v model: AL vs CNR for IN=12,48,96,132

4.4 5G-NR based IoT Performance over TDL-iii

4.4.1 CNR vs BLER

This section evaluates the 5G-NR based IoT air interface with the four FEC scheme with the indoor channel model i.e. TDL-iii, described by the ITU as that suitable for Urban Macro (UMa) environment scenario with high connections density. In fig.4.6,4.7,4.8 and4.9 four configurations are reported, respectively IN=12 bit case with AL=1 and AL=16, and finally IN=132 bit case with AL=1 and AL=16. Some code curves do not achieve the BLER target, but although they are incomplete are easy to foresee the CNR values for 1% BLER. The CNR comparison between this indoor model and outdoor model shows how link parameters involved in indoor scenario widely impact on the CNR performance. Generally, indoor scenario CNR values lose on average 12 dB with respect to CNR valuses in outdoor scenario. Furthermore, it is evident, comparing the previous evaluations, that gain margin of 5G-NR codes with respect to LTE codes is decreased. Moreover, all codes under evaluation perform roughly similarly in cases of IN=132 bit and AL=1, fig.4.8. Same conclusion has been extracted when IN=12 and AL=1, except for Turbo code that is far from the rest of codes performance, fig.4.6 However, the 5G-NR codes show their good capabilities in case of smallest and biggest input length and AL=16, fig.4.7 and 4.9. In the first case, Polar code outperforms the rest of codes, achieving CNR =-11.5 dB while in the second case, LDPC achieves the lowest CNR for 1% BLER, about -4.5 dB.

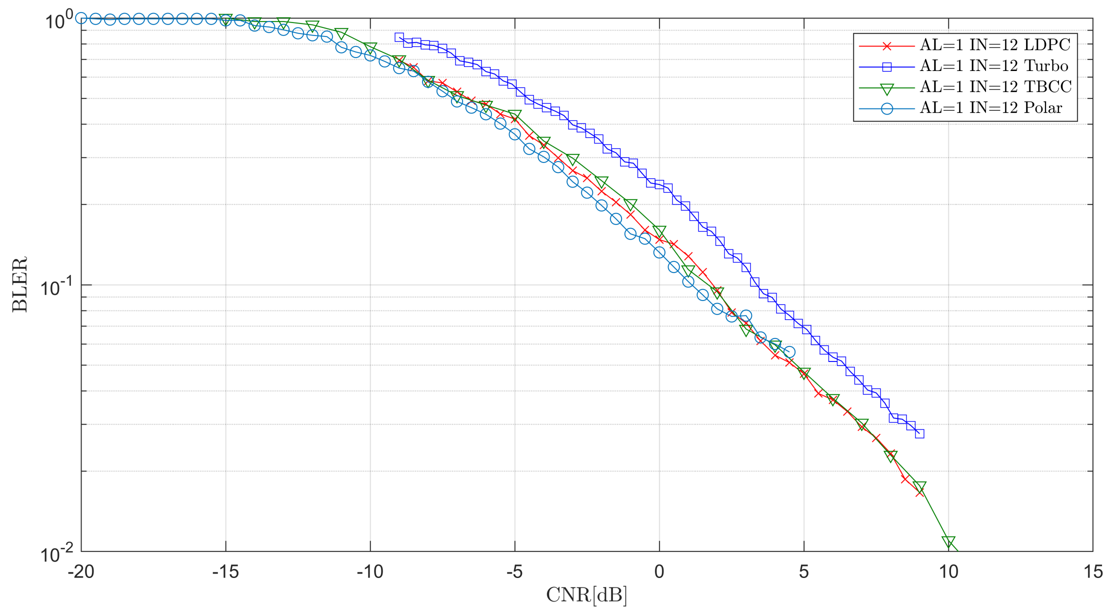

Figure 4.6: TDL-iii model: CNR vs BLER for IN=12 and AL=1

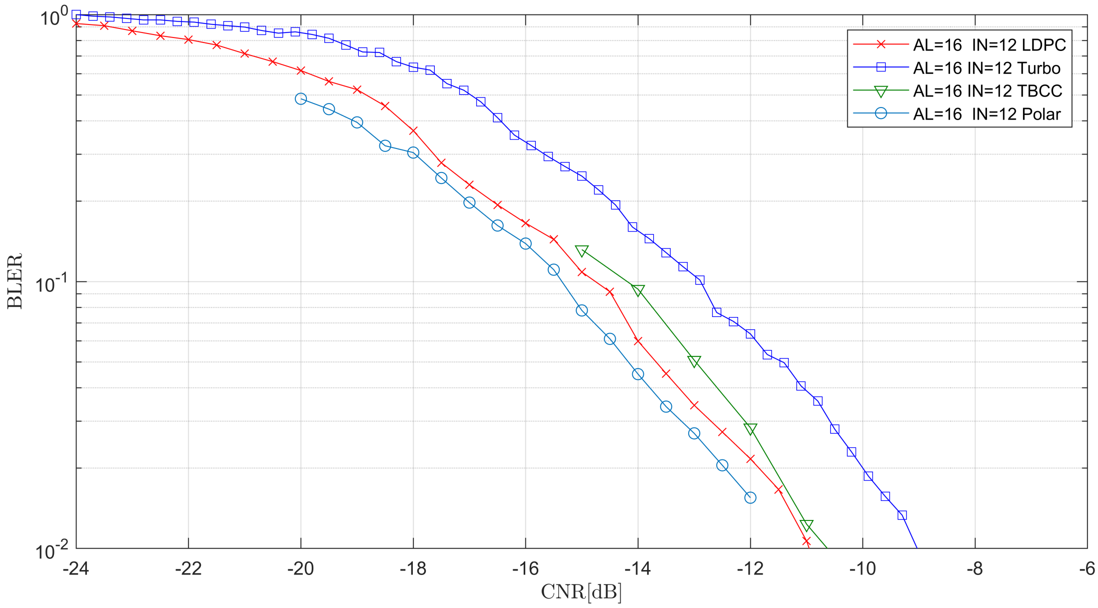

Figure 4.7: TDL-iii model: CNR vs BLER for IN=12 and AL=16

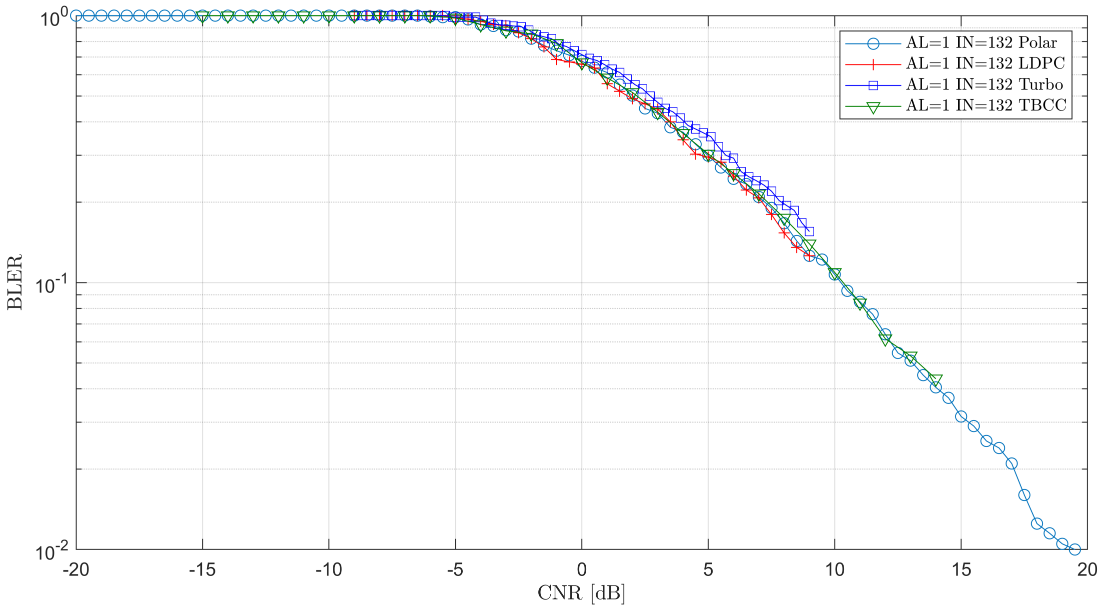

Figure 4.8: TDL-iii model: CNR vs BLER for IN=132 and AL=1

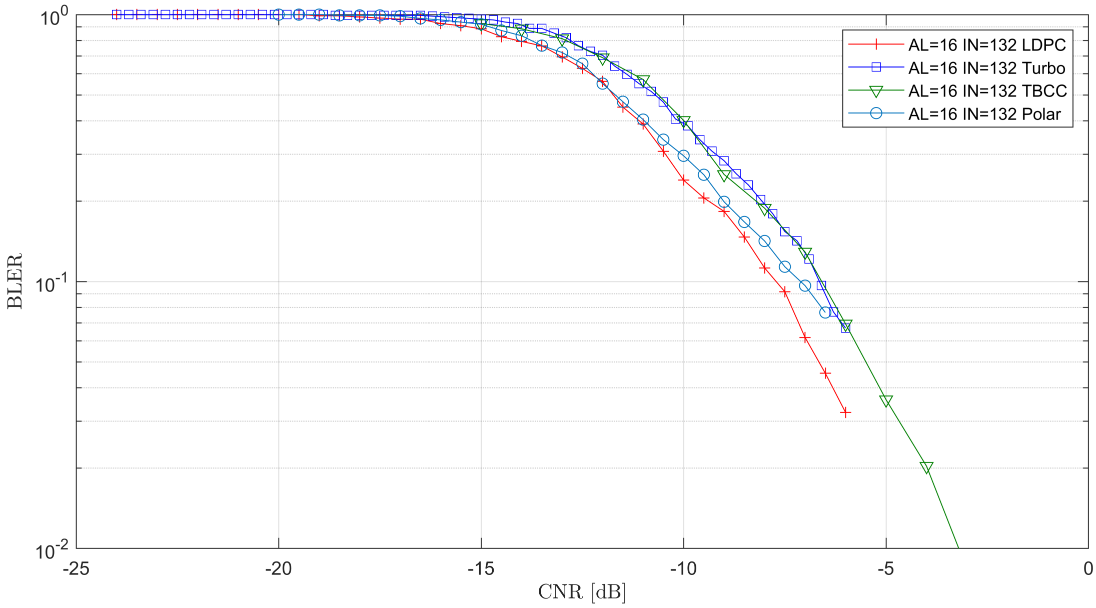

Figure 4.9: TDL-iii model: CNR vs BLER for IN=132 and AL=16

4.5 Link Budget

Link budget is very important to understand how much coverage a telecommunication system can actually provide. *Maximum Coupling Loss (MCL)* is a very common measure to describe the amount of coverage a system, or design, can support because take into account parameters over the link between the UE antenna ports and the base station antenna ports, i.e. antenna gains, path loss, shadowing, body loss, etc. Basically, MCL is defined as the limiting value of the coupling loss at which a service can be delivered, and therefore defines the coverage of the service. In addition, this measure is really useful because is independent of frequency and environment factor. The main goal of link budget evaluation is to show that the 5G-NR based IoT system could support extremely deep coverage condition at 164 dB MCL with at least a data rate of 160 bps, as it is specified in [26]. In particular, in this investigation, it has been evaluated the PDSCH performance, considering the repetitions (AL) that have the aim to achieve a coverage enhancement of 17 dB with respect to the 5G-NR (Rel' 15) MCL target of 143 dB. Consequently, in the MCL computation will be taken into account the downlink parameters defined in the technical report [26]. The following tab.4.2 summarizes how MCL is calculated:

Note The required CNR is a measure of how much noise the design (e.g. modulation, coding rate, coding type, transmission mode, and diversity scheme) can

MCL Input	**Value**
Transmitter	
(1) Max Tx power(dBm)	PA power of eNB
Receiver	
(2) Thermal noise density (dBm/Hz)	*Constant -174*
(3) Receiver noise figure (dB)	depends on LNA
(4) Interference margin (dB)	*considered 0*
(5) Occupied channel bandwidth (Hz)	Bandiwidth of signal
(6) Effective noise power = (2) + (3) + (4) + 10 log(5) (dBm)	*calculated*
(7) Required CNR (dB)	value comes from link simulation
(8) Receiver sensitivity = (6) + (7) (dBm)	*calculated*
(9) Baseline MCL = (1) - (8) (dB)	*calculated*
(10) Target MCL (dB)	164

Table 4.2: MCL calculation

tolerate and still work within a certain performance. i.e. CNR value required to achieve 1% BLER.

4.5.1 Evaluation of six configurations

The main goal of the evaluation is to show that the 5G-NR based IoT system could support extremely deep coverage condition at 164 dB MCL with at least a data rate of 160 bps. The achievable MCL is highly dependent on the number of repetition. The higher the number of repetition, the higher is MCL. Conversely, the double of repetition corresponds to the half of data rate. In addition, the repetitions are in time domain, thus the latency rises significantly. However, latency is not a key performance indicator for IoT applications. First of all, knowing that 1 subframe lasts 1 ms, the data rate formula can be derived as follows:

$$datarate = \frac{IN}{AL \cdot 1ms}[bps]$$

Each configuration achieves different performance. Here, six configurations are evaluated for each FEC scheme with LOS and NLOS channel models:

1. TDL-v model: IN=12, AL=1 achieves 12 kbps
2. TDL-v model: IN=12, AL=2 achieves 6 kbps

3. TDL-v model: IN=132, AL=1 achieves 132 kbps
4. TDL-v model: IN=132, AL=8 achieves 16.5 kbps
5. TDL-iii model: IN=132, AL=1 achieves 132 kbps
6. TDL-iii model: IN=132, AL=16 achieves 8.25 kbps

As can be seen, all these configurations fulfill the data rate requirement, so the aim in the next part will be focused on the coverage target. In the first configuration, tab. 4.3, it has been established that it is not possible to reach the target coverage target of MCL = 164 dB without any repetition for every FEC scheme. In particular, Polar code approaches more than other, but in order to guarantee the quality of service, all FEC schemes need one repetition more.

Table 4.3: Link Budget with TDL-v: IN=12, AL=1

Inner coding	**Polar**	**LDPC**	**Turbo code**	**TBCC**
Transmitter				
(1) Max Tx power(dBm)	46	46	46	46
Receiver				
(2) Thermal noise density (dBm/Hz)	-174	-174	-174	-174
(3) Receiver noise figure (dB)	9	9	9	9
(4) Interference margin (dB)	0	0	0	0
(5) Occupied channel bandwidth (Hz)	180000	180000	180000	180000
(6) Effective noise power = (2) + (3) + (4) + 10 log(5) (dBm)	-112.5	-112.5	-112.5	-112.5
(7) Required CNR (dB)	-5.2	-4.7	-3.1	-4.2
(8) Receiver sensitivity = (6) + (7) (dBm)	-117.7	-117.2	-115.6	-116.7
(9) Baseline MCL = (1) - (8) (dB)	163.7	163.2	161.6	162.7
(10) Target MCL	164	164	164	164
Required Gain = (10)-(9) (dB)	0.3	0.8	3.4	2.3

Tab.4.4 shows that small data length (12bits) just need one repetition more for achieving the MCL target. However, from the formula shown above, the data rate halves due to double of the transmission time of the same amount of information. Here as well, the polar code keeps outperforming than other coding schemes, amply exceeding the coverage target (+ 2.8 dB). Obviously, the repetitions in time lead 3 dB coverage improvement for each FEC scheme, leaving unvaried the differences of coverage among them.

Table 4.4: Link Budget with TDL-v: IN=12,AL=2

Inner coding	**Polar**	**LDPC**	**Turbo code**	**TBCC**
Transmitter				
(1) Max Tx power(dBm)	46	46	46	46
Receiver				
(2) Thermal noise density (dBm/Hz)	-174	-174	-174	-174
(3) Receiver noise figure (dB)	9	9	9	9
(4) Interference margin (dB)	0	0	0	0
(5) Occupied channel bandwidth (Hz)	180000	180000	180000	180000
(6) Effective noise power = (2) + (3) + (4) + 10 log(5) (dBm)	-112.5	-112.5	-112.5	-112.5
(7) Required CNR (dB)	-8.4	-7.6	-6.1	-7.3
(8) Receiver sensitivity = (6) + (7) (dBm)	-120.8	-120.1	-118.6	-119.8
(9) Baseline MCL = (1) - (8) (dB)	166.8	166.1	164.6	165.8
(10) Target MCL	164	164	164	164

In the following tab. 4.5, the MCL calculation is computed taking into account the maximum input length IN under evaluation, 132 bit. Initially, the assessing of performance has been carried out without any repetition, proving that the MCL achieved is far from the target. At least 7.6 dB CNR gain is needed to allow LDPC code achieve the target MCL. Consequently, 8 repetitions are required to gain 9 dB and satisfy the requirement.

The tab.4.6 proves that the repetitions increment(AL=8) leads to the accomplishing of objective for all the FEC schemes.

The last two evaluations are carried out using the indoor model TDL-iii. The tab.4.7 provides information about the assessing of performance without any repetition and IN=132 bit. It has been established that it is not possible to reach the target coverage target of MCL = 164 dB without any repetition for every FEC scheme. The next tab.4.8 shows the performance improvement using 16 repetitions. Nevertheless, it is evident that more than 16 repetitions are needed to achieve the MCL target in this scenario. However, LDPC scheme really approaches to the MCL target and 32 repetitions may be sufficient to guarantee the coverage.

Table 4.5: Link Budget with TDL-v: IN=132, AL=1

Inner coding	**Polar**	**LDPC**	**Turbo code**	**TBCC**
Transmitter				
(1) Max Tx power(dBm)	46	46	46	46
Receiver				
(2) Thermal noise density (dBm/Hz)	-174	-174	-174	-174
(3) Receiver noise figure (dB)	9	9	9	9
(4) Interference margin (dB)	0	0	0	0
(5) Occupied channel bandwidth (Hz)	180000	180000	180000	180000
(6) Effective noise power = (2) + (3) + (4) + 10 log(5) (dBm)	-112.5	-112.5	-112.5	-112.5
(7) Required CNR (dB)	2.3	2.1	2.8	3.1
(8) Receiver sensitivity = (6) + (7) (dBm)	-110.2	-110.4	-109.7	-109.4
(9) Baseline MCL = (1) - (8) (dB)	156.2	156.4	155.7	155.4
(10) Target MCL	164	164	164	164
Required Gain = (10)-(9) (dB)	7.8	7.6	8.3	8.6

Table 4.6: Link Budget with TDL-v: IN=132, AL=8

Inner coding	**Polar**	**LDPC**	**Turbo code**	**TBCC**
Transmitter				
(1) Max Tx power(dBm)	46	46	46	46
Receiver				
(2) Thermal noise density (dBm/Hz)	-174	-174	-174	-174
(3) Receiver noise figure (dB)	9	9	9	9
(4) Interference margin (dB)	0	0	0	0
(5) Occupied channel bandwidth (Hz)	180000	180000	180000	180000
(6) Effective noise power = (2) + (3) + (4) + 10 log(5) (dBm)	-112.5	-112.5	-112.5	-112.5
(7) Required CNR (dB)	-7.7	-8.1	-7	-6.4
(8) Receiver sensitivity = (6) + (7) (dBm)	-120.2	-120.6	-119.5	-118.9
(9) Baseline MCL = (1) - (8) (dB)	166.2	166.6	165.5	164.9
(10) Target MCL	164	164	164	164

Table 4.7: Link Budget with TDL-iii: IN=132, AL=1

Inner coding	**Polar**	**LDPC**	**Turbo code**	**TBCC**
Transmitter				
(1) Max Tx power(dBm)	46	46	46	46
Receiver				
(2) Thermal noise density (dBm/Hz)	-174	-174	-174	-174
(3) Receiver noise figure (dB)	9	9	9	9
(4) Interference margin (dB)	0	0	0	0
(5) Occupied channel bandwidth (Hz)	180000	180000	180000	180000
(6) Effective noise power = (2) + (3) + (4) + 10 log(5) (dBm)	-112.5	-112.5	-112.5	-112.5
(7) Required CNR (dB)	19.3	19.2	19.5	19.3
(8) Receiver sensitivity = (6) + (7) (dBm)	-93.2	-93.3	-93	-93.2
(9) Baseline MCL = (1) - (8) (dB)	139.2	139.9	139.5	139.2
(10) Target MCL	164	164	164	164

Table 4.8: Link Budget with TDL-iii: IN=132, AL=16

Inner coding	**Polar**	**LDPC**	**Turbo code**	**TBCC**
Transmitter				
(1) Max Tx power(dBm)	46	46	46	46
Receiver				
(2) Thermal noise density (dBm/Hz)	-174	-174	-174	-174
(3) Receiver noise figure (dB)	9	9	9	9
(4) Interference margin (dB)	0	0	0	0
(5) Occupied channel bandwidth (Hz)	180000	180000	180000	180000
(6) Effective noise power = (2) + (3) + (4) + 10 log(5) (dBm)	-112.5	-112.5	-112.5	-112.5
(7) Required CNR (dB)	-1.6	-4.4	-3	-3.2
(8) Receiver sensitivity = (6) + (7) (dBm)	-114.1	-116.9	-93	-93.2
(9) Baseline MCL = (1) - (8) (dB)	160.1	162.9	161.5	161.7
(10) Target MCL	164	164	164	164

Chapter 5

Conclusion

Whereas 3GPP has recently announced the 5G NR Rel'15, which is mainly focused on enhanced Mobile Broad-Band (eMBB) family use case within IMT-2020 context, the next Rel'16 will be designed to cover the Ultra-Reliable Low Latency Communications (URLLC) family. Thus, there will be no solution of 5G-NR for the massive Machine Type Communications (mMTC) before Rel'17 (2022). This thesis has dealt with the design and evaluation of different Forward Error Correction (FEC) schemes in order to evaluate the performance of potential 5G-NR based IoT 3GPP system. In particular, the coverage extension, one of the required gains compared with baseline 3GPP systems, has been analysed. Four FEC schemes have been evaluated. The 5G-NR inner codes *Low-Density Parity-Check (LDPC)* (used for data) and *Polar code* (used for control) performance have been calculated and they have been compared with those employed in LTE *Turbo-code* (data) and *Tail Biting Convolutional Code (TBCC)* (control) . The performance evaluation has been carried out through an ad-hoc link-level simulator derived by the 5G-NR Physical Layer simulator of UPV and the 5G Library Toolbox of Matlab®. The evaluations have been performed in terms of Block Error Rate (BLER) for different information block lengths and number of repetitions, under ideal (AWGN) and realistic channel models (TDL-v for outdoor scenario and TLD-iii for indoor scenario characterized by high connections density). In general, it has been seen that Polar coding outperforms the rest of FEC schemes under evaluation, followed by LDPC. It has also been observed that LTE-codes (Turbocode and TBCC) perform worse than 5G-NR codes (Polar and LDPC). However, it has been shown that the performance highly depends on the associated input length. The comparison of 5G-NR codes showed that for short information block length, up to 96 bits, the required Carrier-to-Noise Ratio (CNR) to achieve a Block Error Rate BLER = 10^{-2} is lower with Polar code, but beyond LDPC outperforms Polar. Same conclusion have been extracted between the LTE codes, but the exchange is observed at a shorter information length. TBCC outperforms Turbo code, but the latter surpasses the former from 48 bits. Regarding the impact of the AL, it has been proved that doubling the number of repetitions, increased the performance around 3 dB at the expense halving the overall data-rate. After these evaluations, a link-budget analysis has been conducted in order to estimate the Maximum Coupling Loss (MCL) that the different configurations can actually provide. The goal of evaluation was to show that the downlink channel of 5G-NR based IoT system under evaluation could support extremely deep coverage condition at 164 dB MCL with at least a data rate of 160 bps as it is defined by ITU. It has been established that the data rate condition is always respected regardless of the block length. However, it is not possible to reach the target coverage target of MCL = 164 dB without any repetition for every FEC scheme and regardless of the block length. It has been proved that, in case of TDL-v channel model, whereas small block length (12 bits) just needed two repetitions for achieving the target MCL, bigger block lengths (132 bits) needed at least eight repetitions. Regarding the TDL-iii channel model, it has been estimated that the FEC schemes lost on average 12 dB with respect to the CNR values requested for TLD-v channel model for achieving 1%BLER. Furthermore,it has been proved that, for bigger block lengths (132 bits) are not sufficient eight repetitions any more, but probably at least thirty-two. Future work will include a further evaluation of the system with bigger information data length and higher number of repetitions, as well as the evaluation through a system level simulator, where other characteristics of the system (such as radiation patterns, UEs interferences) are also taken into account.

Appendix A

Summary tables

In this appendix, the CNR values to achieve 1% BLER (equal to 10^{-2}) for every inner coding and channel model are reported in the following tables.

A.1 AWGN model

Polar	**AL**				
IN	1	2	4	8	16
12	-5,497695853	-8,658444023	-11,67552182	-14,4459203	-17,57685009
24	-3,806925996	-6,937855787	-10,37713472	-13,12855787	-16,21204934
36	-2,881878558	-6,178842505	-8,930265655	-12,2983871	-15,23956357
48	-2,19402277	-5,396110057	-8,455882353	-11,44449715	-14,57542694
60	-1,482447818	-4,779411765	-7,7443074	-10,89895636	-13,95872865
72	-0,391366224	-4,162713472	-7,269924099	-10,23481973	-13,08111954
84	-0,083017078	-3,522296015	-6,605787476	-9,523244782	-12,7016129
96	0,773244782	-2,95540797	-6,086337761	-9,10341556	-12,26280835
108	1,057874763	-2,414611006	-5,630929791	-8,591081594	-11,60815939
120	1,712523719	-2,04459203	-5,147058824	-8,306451613	-11,26660342
132	2,129981025	-1,832068311	-4,803605313	-7,911764706	-10,88330171

Table A.1: Polar code: CNR values for 1% BLER with AWGN model

LDPC	**AL**				
IN	1	2	4	8	16
12	-4,69259962	-7,614800759	-10,78368121	-13,74383302	-16,77988615
24	-3,715437788	-6,653225806	-9,302995392	-12,81682028	-15,40898618
36	-2,502371917	-5,751897533	-8,740512334	-11,91888046	-14,64658444
48	-1,672201139	-4,85056926	-7,957779886	-11,11242884	-14,02988615
60	-1,065668203	-4,406682028	-7,517281106	-10,45506912	-13,45046083
72	-0,343927894	-3,901802657	-6,985294118	-9,997628083	-13,00996205
84	-0,035578748	-3,45113852	-6,510910816	-9,712998102	-12,51185958
96	0,574003795	-2,898481973	-6,143263757	-9,24573055	-12,17741935
108	1,086337761	-2,528462998	-5,716318786	-8,818785579	-11,66508539
120	1,513282732	-2,129981025	-5,488614801	-8,562618596	-11,69354839
132	2,078611898	-1,766997167	-5,145184136	-8,183427762	-11,17917847

Table A.2: LDPC code: CNR values for 1% BLER with AWGN model

Turbo	**AL**				
IN	1	2	4	8	16
12	-3,119070209	-6,226280835	-9,14373814	-12,25094877	-15,14468691
24	-2,526091082	-5,585863378	-8,621916509	-11,53937381	-14,57542694
36	-1,387571157	-4,447343454	-7,483396584	-10,40085389	-13,50806452
48	-1,008064516	-3,996679317	-6,985294118	-10,06878558	-13,00996205
60	-0,201612903	-3,261385199	-6,226280835	-9,357210626	-12,27466793
72	-0,011859583	-2,976755218	-6,012808349	-9,00142315	-12,13235294
84	0,830170778	-2,300759013	-5,374762808	-8,534155598	-11,38045541
96	1,200189753	-2,158444023	-5,20398482	-8,221062619	-11,15275142
108	1,769449715	-1,589184061	-4,691650854	-7,623339658	-10,69734345
120	2,082542694	-1,418406072	-4,549335863	-7,537950664	-10,49810247
132	2,680265655	-1,019924099	-4,122390892	-7,025616698	-10,0711575

Table A.3: Turbo code: CNR values for 1% BLER with AWGN model

TBCC	**AL**				
IN	1	2	4	8	16
12	-4,5028463	-7,311195446	-10,46110057	-13,4971537	-16,36242884
24	-3,047912713	-6,036527514	-9,09629981	-12,15607211	-15,04981025
36	-1,838235294	-4,89800759	-7,934060721	-10,94639469	-14,00616698
48	-1,008064516	-4,091555977	-7,151328273	-10,11622391	-13,19971537
60	-0,249051233	-3,261385199	-6,392314991	-9,428368121	-12,36954459
72	0,431688805	-2,642314991	-5,687855787	-8,704933586	-11,72201139
84	0,887096774	-1,947004608	-4,988479263	-8,099078341	-11,00230415
96	1,440092166	-1,475332068	-4,691650854	-7,708728653	-10,49810247
108	2,054079696	-1,105313093	-4,093927894	-7,167931689	-10,15654649
120	2,623339658	-0,649905123	-3,69544592	-6,712523719	-9,786527514
132	3,029953917	-0,771889401	-3,744239631	-6,826375712	-9,957305503

Table A.4: TBCC code: CNR values for 1% BLER with AWGN model

A.2 TDL-v model

Polar	AL				
IN	1	2	4	8	16
12	-5,218216319	-8,462998102	-11,46110057	-14,51612903	-17,38140417
24	-3,85092068	-7,126416431	-10,06550992	-13,16395184	-16,01451841
36	-2,912535411	-6,081798867	-8,914660057	-12,15474504	-15,23548159
48	-2,00426945	-5,277514231	-8,337286528	-11,39705882	-14,52798861
60	-1,283640227	-4,665368272	-7,657577904	-10,61437677	-13,76593484
72	-0,557719547	-3,974858357	-7,091005666	-9,976983003	-13,12854108
84	0,102691218	-3,48796034	-6,356232295	-9,670679887	-12,5601983
96	0,630929791	-2,983870968	-5,887096774	-9,131878558	-12,09203036
108	1,143767705	-2,489376771	-5,570113314	-8,693342776	-11,45538244
120	1,65368272	-2,021954674	-5,123937677	-8,247167139	-11,03045326
132	2,310246679	-1,731499051	-4,663187856	-7,765654649	-10,78273245

Table A.5: Polar code: CNR values for 1% BLER with TDL-v model

LDPC			AL		
IN	1	2	4	8	16
12	-4,731973435	-7,625711575	-10,51944972	-13,74525617	-16,56783681
24	-3,54601518	-6,510910816	-9,570683112	-12,63045541	-15,57163188
36	-2,661290323	-5,725806452	-8,85483871	-11,62903226	-14,62903226
48	-1,842979127	-5,10199241	-7,934060721	-11,06499051	-13,91129032
60	-0,90370019	-4,518500949	-7,279411765	-10,43880455	-13,37049336
72	-0,547912713	-3,849620493	-6,994781784	-9,940702087	-12,84392789
84	0,061669829	-3,422201139	-6,39373814	-9,55313093	-12,43927894
96	0,642314991	-2,909867173	-5,915559772	-9,040796964	-12,08064516
108	1,137571157	-2,585388994	-5,778937381	-8,767552182	-11,67077799
120	1,666982922	-2,158444023	-5,403225806	-8,460151803	-11,34629981
132	2,168880455	-1,607210626	-5,098671727	-8,115749526	-11,07590133

Table A.6: LDPC: CNR values for 1% BLER with TDL-v model

Turbo	**AL**				
IN	1	2	4	8	16
12	-3,166508539	-6,131404175	-9,025142315	-12,01375712	-15,00237192
24	-2,471537002	-5,486717268	-8,515180266	-11,67647059	-14,61195446
36	-1,330645161	-4,589658444	-7,336337761	-10,58111954	-13,34203036
48	-0,889468691	-4,006166983	-6,980550285	-9,89800759	-13,02893738
60	-0,049810247	-3,15227704	-6,183586338	-9,14373814	-12,17504744
72	0,04459203	-2,926944972	-5,915559772	-8,989563567	-11,84155598
84	0,778937381	-2,329222011	-5,266603416	-8,323529412	-11,24383302
96	1,308349146	-1,987666034	-5,078747628	-8,20398482	-11,00474383
108	1,884250474	-1,512333966	-4,643263757	-7,565464896	-10,43074004
120	2,130929791	-1,322580645	-4,377609108	-7,470588235	-10,29791271
132	2,795066414	-0,924098672	-3,865275142	-7,015180266	-10,01328273

Table A.7: Turbo code: CNR required to achieve a BLER of 10^{-2} with TDL-v model

TBCC	**AL**				
IN	1	2	4	8	16
12	-4,281309298	-7,388519924	-10,30597723	-13,43690702	-16,52039848
24	-2,929316888	-6,178842505	-9,072580645	-11,87144213	-14,97865275
36	-1,980550285	-4,99288425	-7,862903226	-10,99383302	-13,93500949
48	-0,913187856	-3,949240987	-6,748102467	-10,13994307	-13,05740038
60	-0,201612903	-3,166508539	-6,273719165	-9,238614801	-12,20351044
72	0,517077799	-2,642314991	-5,317836812	-8,64800759	-11,4373814
84	0,94402277	-1,845351044	-5,090132827	-8,078747628	-10,89658444
96	1,712523719	-1,646110057	-4,350094877	-7,509487666	-10,52656546
108	2,054079696	-1,019924099	-3,951612903	-7,082542694	-10,0711575
120	2,537950664	-0,621442125	-3,581593928	-6,740986717	-9,615749526
132	3,135673624	-0,052182163	-3,154648956	-6,456356736	-9,10341556

Table A.8: TBCC: CNR values for 1% BLER with TDL-v model

A.3 TDL-iii model

In the following table, not valid (N.V.) values refer to all those CNR measurements largely higher than 20 dB.

Polar	**AL**				
IN	1	2	4	8	16
12	10,46040516	8,913443831	3,977900552	-5,672191529	-10,31307551
24	14,95395948	8,76611418	2,283609576	-4,272559853	-9,355432781
36	15,54327808	11,63904236	6,482504604	-3,462246777	-8,32412523
48	16,05893186	12,37569061	4,788213628	-0,810313076	-7,73480663
60	16,05893186	12,37569061	4,788213628	-0,810313076	-7,73480663
72	19,74217311	16,79558011	11,56537753	3,241252302	-3,535911602
84	N.V.	17,01657459	11,34438306	7,661141805	-3,388581952
96	N.V.	N.V.	13,40699816	7,88213628	-1,767955801
108	N.V.	N.V.	14,33333333	5,598526703	-0,73664825
120	18,78453039	16,05893186	11,04972376	8,76611418	-0,2946593
132	19,37384899	17,16390424	12,00736648	6,850828729	-1,620626151

Table A.9: Polar code: CNR values for 1% BLER with TDL-iii model

LDPC	**AL**				
IN	1	2	4	8	16
12	10,78036053	4,637096774	-0,343927894	-6,653225806	-10,97011385
24	12,34108159	6,197817837	1,714895636	-4,793643264	-9,342979127
36	13,53652751	7,559297913	2,013757116	-3,631404175	-8,446394687
48	14,34331797	8,289848197	3,04316888	-2,834440228	-7,416982922
60	15,2016129	9,452087287	3,474857685	-2,170303605	-6,918880455
72	16,08870968	9,385673624	4,271821632	-1,506166983	-6,487191651
84	16,19781784	10,15417457	4,869544592	-1,140891841	-5,657020873
96	17,39326376	11,21679317	5,60483871	-0,685483871	-5,201612903
108	18,02419355	11,2168	6,401802657	-0,405597723	-4,954933586
120	18,78795066	11,81451613	6,601043643	-0,139943074	-4,589658444
132	19,21963947	12,01375712	6,833491461	0,059297913	-4,390417457

Table A.10: LDPC: CNR values for 1% BLER with TDL-iii model

Turbo	AL				
IN	1	2	4	8	16
12	11,97580645	6,283206831	1,515654649	-4,888519924	-8,991935484
24	13,18548387	7,777514231	2,440702087	-3,963472486	-8,398956357
36	14,83396584	8,913662239	4,074952562	-2,073055028	-6,883301708
48	15,14705882	9,340607211	4,217267552	-1,816888046	-6,740986717
60	16,34250474	10,42220114	5,441176471	-1,048387097	-5,80170778
72	16,42789374	10,87760911	5,725806452	-0,564516129	-4,947817837
84	17,45256167	11,58918406	6,323529412	0,20398482	-4,549335863
96	17,65180266	11,93074004	6,750474383	0,374762808	-3,951612903
108	18,64800759	12,35768501	7,433586338	0,830170778	-3,666982922
120	18,90417457	12,58538899	7,775142315	1,000948767	-3,69544592
132	19,55882353	13,46774194	8,486717268	1,883301708	-2,95540797

Table A.11: Turbo code: CNR values for 1% BLER with TDL-iii model

TBCC	AL				
IN	1	2	4	8	16
12	10,19829222	5,300991501	-0,116855524	-6,193342776	-10,59135977
24	12,82827324	6,682011331	1,476628895	-4,302407932	-9,422804533
36	13,09392789	8,148016997	2,475212465	-3,834985836	-8,126770538
48	14,84724858	8,360481586	3,55878187	-2,496458924	-6,894475921
60	15,24573055	9,998229462	4,272308782	-1,503186969	-5,964943343
72	16,33491461	11,25	5,428470255	-0,817988669	-5,428470255
84	16,99905123	10,97379603	5,555949008	-0,39305949	-4,961048159
96	17,84914611	12,08038244	6,180949008	0,578966006	-4,229815864
108	18,0085389	12,03080737	7,023725212	0,950779037	-3,957577904
120	18,85863378	13,14093484	7,021954674	1,476628895	-3,15509915
132	19,35009488	13,42776204	7,847025496	1,78470255	-3,201133144

Table A.12: TBCC: CNR values for 1% BLER with TDL-iii model

Bibliography

[1] J.J. Gimenez E. Garro, M. Fuente. Deliverable D3.2. Air Inteface . Technical report, 5G-Xcast, 2018.

[2] M. Sauter. *From GSM to LTE-Advanced Pro and 5*. Wiley, 2017. Chapter 4 - Long Term Evolution (LTE) and LTE-Advanced Pro.

[3] ITU-R. *Recommendation ITU-R M.2083-0: IMT Vision- Framework and overall objectives of the future development of IMT for 2020 and beyond*, 2015.

[4] International Telecommunication Union. IMT Vision – Framework and overall objectives of the future development of IMT for 2020 and beyond. Technical report, ITU-R, 2015.

[5] Havish Kooropaty Balazas Bertenyi, Satoshi Nagata. 5G NR Radio Interface. *Journal of ICT, Vol. 6 1 e 2, 31–58. River Publishers*, 2018.

[6] ITU-R. *Report ITU-R M.2410-0: Minimum requiremets related to technical performance for IMT-2020 radio interface(s)*, 2017.

[7] Joe Barrett. Outlining the Roadmap to 5G. *Journal of ICT, Vol. 6 1 e 2, 1–14. River Publishers*, 2018.

[8] G.P. Hancke Adnan G.A. Akpakwu, B.J. Silva and M.Abu-Mahfouz. A survey on 5g networks for the internet of things: Communication technologies and challenges. *IEEE*, 2017.

[9] ITU-R. *Report ITU-R M.2412-0: Guidelines for evaluation of radio interface technologies for IMT-2020*, 2017.

[10] M. Boldi P. Marsch, O. Queseth. *5G system design, architecture and funcional considerations and long term research*. Wiley, 2018.

[11] Ericsson. Cellular Networks for Massive IoT: Enabling Low Power Wide Area Applications. Technical report, Ericson, 2016.

[12] E. Berthelsen and J. Morrish. Forecasting the Internet of Things revenue opportunity. *IEEE*, 2016.

[13] 3GPP. *TS 45.820 v2.1.0: Cellular System Support for Ultra Low Complexity and Low Throughput Internet of Things*, 2015.

[14] A. Furuskär S. Parkvall, E. Dahlman and M. Frenne. NR: The New 5G Radio Access Technology. *IEEE Communications Standards Magazine*, 2017.

[15] 3GPP. *TS 38.213 v15.1.0: Physical Layer Procedures for Control*, 2018.

[16] *3GPP TS 38.331 v.15.1.0: NR. Radio Resouce control (RRC), Protocol Specification*, 2015.

[17] C.E.Shannon. A mathematical theory of communication. *The Bell System Technical Journal*, vol. 27(no. 3):pp. 379–423, 1948.

[18] E. Arikan. Channel Polarization:a method for constructing capacity-achieving codes doe symmetric binary-input memoryless channels. *IEEE Transactions on Information Theory,vol.55,no.7,pp.3051-3073*, 2009.

[19] Tal an A.Vardy. List deconding of polar codes. *IEEE Trans. Inf. Theory*, vol. 61(no. 5):pp. 2213–2226, 2015.

[20] S.Schwarz B.Tahir. BER comparison between Convulutional,Turbo,LDPC and POlar code . *IEEE*, 2017.

[21] R.G.Gallager. *Low Density Parity Check Codes.* PhD thesis, MIT Cambrige, 1960.

[22] K.Yang S.Myung and Y.Kim. Lifting methods for quasi-cyclic LDPC codes. *IEEE Communications Letters, vol. 10, no. 6, pp. 489–491*, 2006.

[23] H. Jin D. Divsalar and R. McEliece. Coding theorems for turbo-like codes. *IEEE Communications Letters*, vol. 10(no. 6):pp. 489–491, 1998.

[24] W. Xu O. Iscan, D. Lentner. A Comparison of Channel Coding Schemes for 5G Short Message Transmission . *Huawei Technologies Duesseldorf GmbH*, 2016.

[25] 3GPP. *TS 38.901 v15.0.0: Physical Study on channel model for frequencies from 0.5 to 100 GHz*, 2018.

[26] 3GPP. *3GPP TS 38.913 v14.3.0:Study on Scenarios and Requirements for Next Generation Access Technologies*, 2018.